Cleaner Environmental Systems 22 (2026) 100462

Contents lists available at ScienceDirect

Cleaner Environmental Systems

journal homepage: www.journals.elsevier.com/cleaner-environmental-systems

Life-cycle environmental and social trade-offs in concrete road frame systems

Andrés Ruiz-Vélez [a], Antonio J. Sánchez-Garrido [b,*], Julián Alcalá [a], Víctor Yepes [a]

[a] Dept. of Construction Engineering, Universitat Politècnica de València, Valencia, 46022, Spain
[b] Institute of Concrete Science and Technology (ICITECH), Universitat Politècnica de València, Valencia, 46022, Spain

ARTICLE INFO

Keywords:
Life cycle
Social LCA
Infrastructure
Concrete
Trade-offs
Sustainability
Cleaner production

ABSTRACT

Life cycle sustainability assessment is increasingly applied to support cleaner production and informed decision-making in infrastructure systems. However, comparative evidence integrating environmental and social dimensions across alternative construction typologies remains limited, particularly for standardized, high-volume road structures. This study evaluates life-cycle environmental and social trade-offs in concrete road frame systems to support sustainability-oriented typology selection. Two widely used reinforced concrete construction systems—precast modular hinged frames and cast-in-place frames—are compared using an integrated environmental Life Cycle Assessment (LCA) and screening-level Social LCA. A total of 50 cost-optimized configurations are analyzed, spanning 8–16 m and soil cover depths of 1–5 m. All systems are assessed within consistent cradle-to-grave boundaries and normalized to a single linear meter of structure to ensure comparability across geometric conditions. Environmental impacts are quantified using the ReCiPe 2016 method, while social performance is evaluated with the PSILCA/SOCA v2 framework. Results show that precast systems reduce greenhouse gas emissions by approximately 9–17% compared to cast-in-place alternatives, with increasing absolute savings for larger spans. Social impacts exhibit scale-dependent behavior: precast frames perform better for smaller configurations, whereas cast-in-place systems show lower social impact scores for larger spans, reflecting differences in labor intensity and supply-chain structure. These findings confirm that no construction typology is universally preferable and that environmental and social life-cycle performance varies with geometric scale. Unlike conventional case-based LCA studies, this work adopts a parametric and optimization-driven approach that reveals how environmental and social impacts evolve with geometric scale and identifies crossover points between structural typologies, providing actionable insights for early-stage infrastructure design.

1. Introduction

Contemporary engineering is increasingly focused on measuring and addressing the ecological consequences arising from technological progress and socio-economic growth. These systems must achieve greater resilience and sustainability, as recent global crises—including the pandemic and geopolitical disruptions—have underscored the fragility of conventional development models. The United Nations' Sustainable Development Goals (SDGs) included in the 2030 Agenda express this global commitment, promoting strategies that ensure environmental protection and societal welfare (Barahmand et al., 2026; WCED, 2015), supported by instruments such as Environmental Product Declarations (EPDs) and ESG metrics for assessing and communicating sustainability outcomes (ISO, 2006a; Božićek et al., 2021).

Their practical application in territorial and urban planning contexts has proven to be fundamental for improving resilience and informing long-term infrastructure decisions (Hack et al., 2025). Broader reviews of sustainable construction trends identify life-cycle thinking, industrialized construction, and integrated environmental–social assessment as central pillars of next-generation infrastructure design (Zajemska et al., 2025). Achieving these objectives requires a systematic understanding of how products and processes generate environmental and social impacts throughout their life cycles (Garcia et al., 2017; Ashraf et al., 2025). Recent studies have also emphasized the importance of incorporating uncertainty-aware and sustainability-oriented material and structural assessments, particularly in concrete-based systems, where

* Corresponding author.
E-mail addresses: aruivel@doctor.upv.es (A. Ruiz-Vélez), ajsangar@doctor.upv.es (A.J. Sánchez-Garrido), jualgon@cst.upv.es (J. Alcalá), vyepesp@cst.upv.es (V. Yepes).

https://doi.org/10.1016/j.cesys.2026.100462
Received 29 January 2026; Received in revised form 28 May 2026; Accepted 29 May 2026
Available online 1 June 2026

variability in material behavior and lifecycle performance plays a critical role in decision-making (Gao et al., 2021, 2023).

The building industry remains a critical component of socioeconomic systems but also constitutes a significant source of global greenhouse gas emissions and the loss of natural resources (García-Segura et al., 2014; Garcia et al., 2022). Material production alone accounts for nearly 9% of annual anthropogenic CO_2 emissions (Labaran et al., 2022). Cement production—a basic element in concrete—generated around 2.3 gigatonnes of CO_2 emissions in 2022 (Pakdel et al., 2021; UNEP, 2022), underscoring embodied carbon as a pivotal metric for evaluating climate-related performance.

Recent studies, including those published in Results in Engineering, demonstrate how recycled aggregates, optimized geometries, and supplementary cementitious materials can substantially reduce embodied emissions (Polo-Mendoza et al., 2023; Firoozi et al., 2024). Similarly, integrating ecological footprint and circular economy perspectives into material design contributes to more sustainable construction practices (Barahmand et al., 2026; Kanwal et al., 2025; Casale et al., 2025). However, achieving a genuinely sustainable transformation requires the concurrent integration of environmental, economic, and social dimensions. Comparative sustainability assessments of conventional and alternative structural systems show that trade-offs differ across environmental and social dimensions. This finding highlights the need for integrated frameworks rather than single-criterion evaluations (Kufner et al., 2025).

Progress toward more sustainable concrete structures has followed two complementary paths. The first focuses on the development of low-impact concretes that incorporate industrial by-products, recycled aggregates, or alternative binders to minimize raw material use and emissions (Imbabi et al., 2012). Once regulatory and industrial frameworks mature, this approach can significantly transform construction practice (Ayarkwa et al., 2022). In this context, recent research has also explored the coupling between material innovation and lifecycle sustainability performance in concrete and composite systems, highlighting the relevance of incorporating alternative materials and structural configurations under varying environmental conditions (Gao, 2025; Zhang et al., 2026).

The second approach applies multi-objective structural optimization, integrating parameters such as geometry, materials, and cost. Advanced metaheuristic algorithms—such as hybrid simulated annealing or evolutionary computation—enable the creation of structures that meet safety requirements while minimizing environmental footprints (Yepes-Bellver et al., 2025). Recent studies have further demonstrated the effectiveness of life-cycle optimization approaches in reducing environmental impacts in both transportation infrastructure and building systems, highlighting their applicability across different concrete structural typologies (Li et al., 2025; Negrín et al., 2023). Incorporating optimization early in the design process can lower life-cycle CO_2 emissions by nearly 10% (Zhu et al., 2025), illustrating the significant influence of design parameters on sustainability outcomes. This sensitivity of environmental performance to structural span and system configuration has likewise been demonstrated in life-cycle assessments of alternative floor systems, confirming geometry as a key driver of embodied impacts (Almulhim et al., 2025). These methods enable performance-based design criteria that balance economic and environmental benefits (Ruiz-Vélez et al., 2023a). Parametric optimization of construction systems has also been shown to reduce embodied carbon while supporting circular design strategies, reinforcing the importance of early-stage design decisions in sustainability outcomes (Al-Obaidy et al., 2022). These advances highlight the relevance of optimization-based approaches across both component and infrastructure scales, where design decisions have long-term environmental and societal implications.

Within this context, transportation infrastructure has emerged as a priority research area due to its material intensity, long lifespan, and critical social function. Prior investigations have explored environmental and economic optimization in composite bridges (Kaveh et al., 2014), pavement management systems (Zulu et al., 2020), and reinforced concrete frames (Ruiz-Vélez et al., 2023b). Evidence from the building sector likewise indicates that adaptable and industrialized construction systems improve constructability, resource efficiency, and long-term flexibility, reinforcing the relevance of modular approaches for sustainability-oriented structural design (Sadafi et al., 2012). This limitation is particularly relevant to road structures, where typological and construction choices determine long-term impacts (More-López et al., 2023; Backes and Traverso, 2024). Although progress has been achieved in bridges (Milić and Bleiziffer, 2024) and building systems (Sánchez-Garrido et al., 2022), comparable evaluations for road frame systems are scarce. A comparative understanding of environmental and social performance across construction typologies is therefore essential to clarify these trade-offs in this infrastructure category. However, existing studies are often limited to isolated case analyses, hindering the systematic evaluation of sustainability trade-offs across design alternatives. Within this context, road frame systems represent a particularly relevant case study due to their widespread use, structural variability, and sensitivity to both geometric and construction-related parameters.

Reinforced concrete structures for roads are among the most common solutions for underpasses and crossings. They are typically constructed as in-situ reinforced concrete frames (ISRCF) or precast reinforced concrete articulated frames (PRCAF), each exhibiting distinct characteristics during their manufacturing, service, and end-of-life phases. Earlier studies have demonstrated that advanced optimization approaches applied to structural columns result in significant reductions in material use (Penadés-Plà et al., 2018). Building on this foundation, Ruiz-Vélez et al. (2023a) used a hybrid multi-objective optimization framework with simulated annealing to evaluate the geometry, material consumption, and environmental performance of 25 standardized ISRCF and PRCAF configurations, with lengths ranging from 8 to 16 m and ground coverages ranging from 1 to 5 m. However, the social performance of these alternative construction typologies remains largely unexplored.

Determining the most suitable typology for a specific geometry has a decisive effect on the overall environmental and social life-cycle performance of road infrastructure. Accordingly, this study conducts a comparative analysis of environmental and social aspects across the life cycle of 50 cost-optimized road frames, in alignment with the methodological framework defined by ISO 14040 and ISO 14044 (ISO, 2006b; ISO, 2006c). By analyzing both environmental and social indicators across multiple configurations, it identifies when precast or cast-in-place alternatives offer superior performance (Meireles et al., 2024; Aghasizadeh et al., 2022). This comparative assessment framework supports typology selection under competing objectives rather than the development of new materials or construction technologies.

Ultimately, the research advances current knowledge by coupling cost optimization with integrated environmental and social assessment for reinforced concrete road frames. This approach enables the systematic evaluation of trade-offs among geometry, construction method, and life-cycle impact, providing decision-support evidence for sustainability-informed infrastructure planning and preliminary design rather than project-specific certification or optimization.

Despite the growing body of literature on life-cycle assessment of concrete structures, the integration of environmental and social dimensions within a unified, design-oriented framework for road frame systems remains limited (Moretti et al., 2017; Barbero et al., 2024). As a result, current LCA studies provide static comparisons that do not capture how sustainability performance evolves across alternative designs or how relative advantages between construction typologies may change with geometric scale. In particular, existing studies tend to focus either on specific case studies or on single structural configurations, without systematically exploring how sustainability trade-offs evolve across a range of optimized design alternatives.

In this context, the study addresses the following research questions.

Specifically: (i) how do environmental and social life-cycle impacts vary between prefabricated and cast-in-place concrete road frame systems across different span lengths; (ii) to what extent do cost-optimized structural configurations influence sustainability-related impacts; and (iii) what trade-offs emerge between environmental and social dimensions when comparing alternative structural typologies. Therefore, this study contributes a design-oriented, parametric, and decision-support framework that bridges the gap between life-cycle assessment methodologies and practical infrastructure typology selection.

The novelty of this work lies in the combined application of environmental and screening-level (PSILCA-based) social life-cycle assessment to a parametric set of 50 cost-optimized structural configurations, enabling a systematic and scalable comparison of design alternatives. This parametric and optimization-driven approach makes it possible to identify how environmental and social impacts evolve with geometric scale and to detect threshold conditions where the relative advantage between structural typologies changes. Importantly, the contribution does not reside in proposing new LCA methods, but in structuring their combined application within a scalable, design-oriented framework that supports comparative interpretation across multiple optimized alternatives.

2. Materials and methods

This research provides a comparative assessment of the environmental and social dimensions associated with optimized reinforced concrete road structures within a sustainability-oriented evaluation framework. The approach is based on the life cycle assessment (LCA) framework standardized by ISO 14040 (2006b) and ISO 14044 (2006c), which structures the process into four main phases: (i) definition of objectives and scope, (ii) collection of input and output data, (iii) evaluating the associated impacts, and (iv) analyzing and interpreting the outcomes.

To obtain an integrated environmental and social assessment overview, two complementary analyses were performed: an Environmental Life Cycle Assessment (E-LCA) and a Social Life Cycle Assessment (S-LCA). Integrating these two dimensions makes it possible to monitor how environmental impacts and social implications evolve across the full life span of cost-optimized reinforced concrete road frames and to compare competing construction typologies under consistent system boundaries and functional units. This perspective aligns with systematic efforts to structure social sustainability indicators in construction projects, particularly regarding labor conditions, community well-being, and value-chain transparency (Rostamnezhad and Thaheem, 2022).

Regarding the environmental evaluation, this research employed the ReCiPe 2016 method for assessing life-cycle impact (Huijbregts et al., 2017), drawing mainly from the BEDEC and Ecoinvent v3.7.1 databases as foundational data sources (Pascual-González et al., 2016; Catalonia Institute of Construction Technology, 2023). These databases provide reliable, high-quality information on material production, energy use, and construction operations representative of European construction contexts and commonly used in infrastructure LCA studies. The social dimension was modeled using the PSILCA database implemented through the SOCA v2 platform, which compiles detailed inventories of socioeconomic processes (GreenDelta, 2013; Navarro et al., 2024; Sánchez-Garrido et al., 2026a). Social impacts were derived using the social impact weighting approach, maintaining alignment with the structure and boundary conditions of the environmental analysis to enable consistent cross-dimensional comparison.

All modelling tasks and numerical processing were executed using the open-source platform OpenLCA (Ciroth, 2007), a reference tool in infrastructure-focused LCA studies due to its adaptability and transparency. The combined use of international standards, reliable databases, and replicable open-source modelling tools guarantees the methodological soundness and reproducibility of this work for comparative infrastructure assessment purposes.

2.1. Objective and study framework

This research aims to analyze how cost-optimized design strategies affect the life-cycle environmental and social performance of reinforced concrete road frames in the context of early-stage infrastructure decision-making. Two structural alternatives—ISRCF and PRCAF—were systematically evaluated through an integrated E-LCA/S-LCA framework. The study encompassed 50 optimized cases derived from 25 parametric combinations, linking spans between 8 and 16 m with cover depths ranging from 1 to 5 m. The joint E-LCA/S-LCA evaluation quantified overall impacts and identified the most favorable alternatives for each geometric and constructive condition rather than optimizing a single configuration. Furthermore, the work pinpointed the life-cycle phases exerting the highest influence on total life-cycle impacts. Because PRCAF systems generally ensure higher dimensional precision and uniform material quality than ISRCF solutions (Richardson, 2003), and their modular production minimizes field operations, both construction approaches were examined comprehensively across all life-cycle stages (Ansah et al., 2021). The system boundaries follow a cradle-to-grave approach, covering material production, transportation, construction, use (including carbonation effects), and end-of-life processes. The life-cycle inventory is primarily based on secondary data obtained from established databases (Ecoinvent, BEDEC, and PSILCA/-SOCA v2), complemented by design-specific calculations derived from the structural optimization process. The geographical representativeness corresponds to European (Spanish) conditions, while temporal representativeness reflects current industrial practices embedded in the selected databases. Within this framework, span length and soil cover are treated as boundary conditions imposed by site requirements rather than as design variables, and the comparative assessment is therefore conducted between structural typologies for each predefined geometric configuration.

The proposed framework extends conventional life-cycle assessment applications by explicitly integrating environmental and social indicators within a comparative, design-oriented approach. Rather than focusing on single case studies or ex-post evaluations, the methodology enables the systematic assessment of multiple optimized design alternatives, supporting early-stage infrastructure decision-making. This approach facilitates the identification of trade-offs between environmental and social dimensions and contributes to bridging the gap between life-cycle assessment methodologies and practical typology selection in road infrastructure systems (Moretti et al., 2017). This contrasts with most S-LCA applications in construction, which are typically retrospective and case-specific, limiting their usefulness for early-stage design comparison and typology selection.

2.1.1. Selection of optimal road frame configuration

Reinforced concrete structures for roads are a standard structural solution in transport infrastructure, as they allow for the separation of levels between intersecting roads. They generally span between 8 and 16 m and are capable of supporting embankments of almost 10 m in height, while maintaining internal clear heights of around 5 m. Their robustness and versatility make them ideal for locations with low bearing capacity soils or where hydraulic factors, such as possible flooding or scouring, require greater structural reliability.

Two dominant design approaches exist: closed, monolithic frames constructed entirely on-site, and modular, open frames assembled from prefabricated U-shaped elements. Prefabricated systems offer operational and sustainability advantages, including shorter installation times, reduced site disturbance, and improved resource utilization. Although ISRCFs have traditionally been the standard solution, recent advances in prefabrication have enhanced the competitiveness of PRCAFs, offering measurable environmental and cost benefits (Ruiz-Vélez et al., 2023b) under certain geometric and logistical conditions.

This research evaluates optimized structural designs for both

typologies. The primary geometric parameters governing ISRCF design are span length (L), overall height (H), and earth cover (HE); in PRCAF systems, the hinge joint height (HH) is an additional defining variable. Fig. 1 illustrates the key geometric features and structural configurations examined in this study for comparative assessment purposes.

2.1.2. Stages involved in the assessment process

The life cycle framework encompasses all activities, from the procurement of raw materials to the management of the structure's end of life. Four successive phases—manufacturing, construction, service, and decommissioning—were modeled, each associated with specific environmental and social implications and defined consistently for both typologies:

- Manufacturing: includes resource extraction, material processing, and the fabrication of concrete and reinforcing steel for both typologies.
- Construction: comprises the transport of materials to the site and assembly processes, differing substantially between prefabricated and on-site casting techniques.
- Use: extends over a 100-year design service life, incorporating periodic maintenance and the influence of concrete carbonation on long-term performance.
- End-of-life: involves dismantling, material sorting, and transportation to recycling or landfill destinations. Steel reinforcement is assumed to be fully recycled, while concrete rubble undergoes complete carbonation before being disposed of.

This breakdown enables the allocation of social and environmental impacts to specific life-cycle stages, resulting in a comprehensive sustainability profile for both construction approaches and facilitating stage-level trade-off analysis between alternatives.

2.1.3. Functional unit definition

Design optimization of each frame type depends on various geometric and mechanical conditions. In line with standard design specifications (CEN, 2013; Ministerio de Fomento, 2011), the functional unit adopted in this study corresponds to one linear meter of road frame. All analyses—structural, environmental, and social—were normalized to this reference unit, ensuring direct comparability between typologies. Consequently, the reported results represent impacts per linear meter of structure, providing a consistent metric for evaluating the life-cycle sustainability of ISRCF and PRCAF systems within an alternatives assessment framework.

2.2. Life-cycle inventory compilation

The life-cycle inventory (LCI) phase systematically quantifies all material inputs, energy consumption, and labor requirements associated with producing one linear meter of each road frame configuration. This dataset provides the quantitative foundation for estimating and comparing the social and environmental impacts of the two structural alternatives: cast-in-place (ISRCF) and precast hinged (PRCAF) concrete frames under harmonized system boundaries and functional units.

2.2.1. Software

To ensure a robust and comprehensive environmental assessment, the E-LCA combined two complementary databases. The Ecoinvent 3.7.1 repository served as the main reference due to its extensive, quality-assured life-cycle datasets (Pascual-González et al., 2016; Frischknecht and Rebitzer, 2005). When specific processes were unavailable, supplementary data were retrieved from the BEDEC database (Catalonia Institute of Construction Technology, 2023) to enhance representativeness for regional construction practices. For the social dimension, the SOCA v2 database (GreenDelta, 2013) was utilized, integrating the PSILCA framework to consistently link social indicators with each process modeled in the environmental inventory through shared activity flows and system structure.

All computations were conducted in OpenLCA (Ciroth, 2007), an open-access platform recognized for its transparency in infrastructure-oriented sustainability studies. The environmental impacts were determined through the ReCiPe 2016 Life Cycle Impact Assessment (LCIA) approach, employing both midpoint and endpoint indicators. Social outcomes were derived using the Weighted Social Impact method at the endpoint level. This methodological alignment allows for internally consistent cross-comparison of environmental and social results between both typologies. Table 1 summarizes the key databases, assessment methodologies, and computational tools employed throughout the study.

2.2.2. Uncertainty

All LCA models inevitably involve a degree of uncertainty due to differences in data sources, regional specificity, and temporal coverage. To strengthen the robustness of the analysis, the Ecoinvent 3.7.1 dataset was supplemented with information from the regional BEDEC database, ensuring a more contextualized and comprehensive representation of local construction conditions. Uncertainty factors were estimated using a genealogical matrix methodology (Ciroth et al., 2016), which assesses parameters such as data reliability, completeness, temporal and spatial alignment, and technological compatibility. Both generic and process-dependent uncertainty factors were incorporated to provide a consistent quantification of variability within the modeled system and to support the comparative interpretation of results rather than the prediction of absolute impact values.

Table 1
Databases and computational tools employed in the life-cycle assessment.

Evaluation	Dataset	Life Cycle Impact Assessment	Perspective	Tool
E−LCA	Ecoinvent 3.7.1 & BEDEC	ReCiPe 2016 (H)	Midpoint Endpoint	OpenLCA
S−LCA	PSILCA − SOCA v2	Weighted Social Impact Method	Endpoint (MRH)	OpenLCA

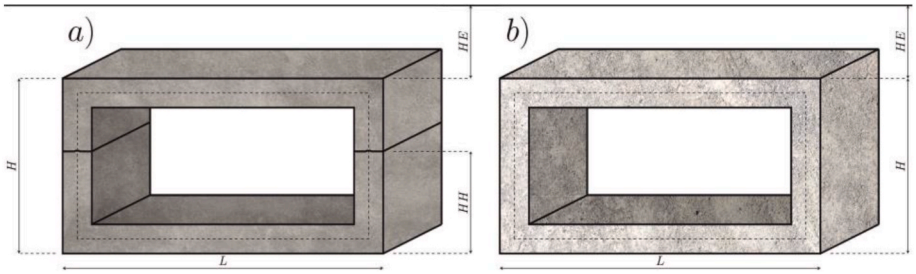

Fig. 1. Structural typologies and geometric descriptors of road frames: (a) precast modular hinged frame (PRCAF); (b) in-situ reinforced concrete frame (ISRCF).

2.2.3. Road frame design

Fifty cost-optimized frame structures were examined, representing 25 geometric combinations typical of road underpasses and crossings. Span lengths ranged from 8 m to 16 m in 2 m increments, and soil cover depths varied between 1 m and 5 m. These configurations capture realistic design variability observed in practice. Although ISRCF and PRCAF alternatives share comparable material specifications (Penadés-Plà et al., 2018; Ruiz-Vélez et al., 2023a), differences in fabrication and installation lead to distinct sustainability profiles (Ruiz-Vélez et al., 2023b) that justify a comparative life-cycle assessment rather than a single-typology evaluation.

The optimization of the structural configurations was formulated as a single-objective cost minimization problem, in which the total construction cost per linear meter was minimized subject to structural safety and serviceability constraints. The design variables included geometric parameters (e.g., slab thicknesses, wall dimensions, and, for PRCAF systems, hinge geometry) as well as reinforcement layouts. All candidate solutions were required to satisfy ultimate and serviceability limit states in accordance with Eurocode 2 provisions (CEN, 2013), including bending, shear, and cracking control, ensuring structural feasibility and compliance with standard design practice. Material strength classes (C25 concrete and B500S steel) were kept constant, while quantities were optimized to achieve minimum cost under these constraints.

The optimization process was conducted independently of the environmental and social assessments; that is, LCA indicators were not included in the objective function but were evaluated a posteriori for each cost-optimal solution. This sequential coupling allows the identification of sustainability implications associated with economically optimal designs, providing a realistic basis for comparison with conventional engineering design practices, where cost-optimal solutions are typically adopted without explicitly accounting for life-cycle environmental and social impacts. This approach also facilitates the reproducibility of the optimization framework, as all design variables, constraints, and evaluation stages are explicitly defined.

All reinforcement designs utilized a C25 concrete grade, combined with B500S reinforcing steel. Although fixed material classes were adopted to ensure consistency across the comparative analysis, the proposed optimization and assessment framework is not restricted to these specific grades. Alternative material scenarios—such as higher-strength concretes, low-clinker binders, or recycled/reused steel—can be incorporated by modifying the corresponding mechanical properties, material quantities, and life-cycle inventory datasets within the same methodological structure. However, variations in material properties and production processes may alter both environmental and social impact magnitudes, and therefore the comparative results should be reassessed for each alternative material scenario. The concrete mix, containing approximately 275 kg/m^3 of cement (with 95% clinker), 165 L/m^3 of water, about 1035 kg/m^3 of coarse aggregates, and 1155 kg/m^3 of sand, was selected to balance mechanical reliability with lower environmental impact. The use of higher-strength concrete would have increased the proportion of cement and, consequently, the associated emissions and costs; therefore, the 25 MPa mix represented the most efficient and sustainable option within the optimization framework adopted. Table 2 details the quantities of material required per linear meter of ISRCF, taking into account burial depths of 1 m and 5 m for each section. Additional components include approximately 11–13 m^2 of geotextile, 0.8–1.6 m^3 of cover concrete, and 62–172 m^2 of formwork per meter of structure.

For precast hinged frames (PRCAF), Table 3 details the corresponding material demands per linear meter. Due to their prefabricated production, PRCAFs eliminate the need for blinding concrete and formwork, but involve 11.59–12.39 m^2 of geotextile, 0.80–1.60 m^3 of leveling sand, and 13.74–39.03 m^3 of reusable steel molds (with an average durability of 150 uses) as modeled in the life-cycle inventory.

2.2.4. Methodological framework for life cycle modeling

Fig. 2 presents the complete life-cycle scheme developed for the assessed road frame systems, structured into four successive phases: raw material manufacturing, on-site construction and assembly, operational service period, and final deconstruction and disposal management. The environmental inventory was primarily based on the Ecoinvent database, with complementary data from BEDEC to capture regional construction processes accurately. This unified structure enabled the incorporation of corresponding social impact data from the SOCA v2 database, ensuring coherence between the environmental and social assessment frameworks and enabling stage-level comparison across typologies. Optimization-based analyses further indicate that construction scheduling and sequencing decisions can materially affect both economic and environmental performance, underscoring the importance of explicitly modeling the construction phase in life-cycle sustainability assessments (Su et al., 2025).

Building on the screening-level social assessment described in Section 2.3, the integrated E-LCA/S-LCA framework is designed to support typology selection by enabling the parallel interpretation of environmental and social indicators across multiple optimized design alternatives. Rather than aggregating results into a single composite score, the framework preserves the multidimensional nature of sustainability performance, allowing decision-makers to identify trade-offs between environmental efficiency and social risk exposure. This approach is particularly relevant in early-stage infrastructure design, where multiple feasible configurations exist and decisions must be made under incomplete information. By structuring results comparatively across typologies and geometric parameters, the framework allows decision-makers to identify trade-offs rather than relying on a single composite score, and to select structural typologies according to project-specific priorities (e.g., minimizing environmental impact vs. reducing social risk exposure).

2.2.4.1. Manufacturing phase. This stage encompasses every preliminary process necessary to obtain construction materials, starting with the extraction of natural resources and continuing through the fabrication of the finished structural elements. The principal materials considered are 25 MPa concrete and B500S reinforcing steel, as previously described. Concrete production entails sourcing and transporting raw aggregates, followed by a series of industrial operations—crushing, grinding, proportioning, and batching—to generate the final mix. Steel reinforcement arises from two complementary supply chains: one based on primary production using the blast oxygen furnace (BOF) pathway from mined ores, and the other from secondary recycling via electric arc furnace (EAF) melting of scrap. The two streams converge in the hot-

Table 2
Quantities of materials required per linear meter of ISRCF, categorized by span range.

Span (m)	Steel (kg)	Concrete (m^3)	Backfill (m^3)	Drain filler (m^3)
16	3313.89–7267.24	40.49–55.84	21.45–115.37	18.91–21.17
14	2641.34–5535.33	31.10–44.10	19.34–104.62	18.05–19.97
12	2034.13–4182.33	23.73–34.07	17.23–93.87	17.21–18.81
10	1556.60–3055.06	17.26–25.38	15.11–83.12	16.39–17.68
8	1223.84–2046.48	12.91–20.24	13.00–72.37	15.58–16.58

Table 3
Quantities of materials required per linear meter of PRCAF, categorized by span range.

Span (m)	Steel (kg)	Concrete (m^3)	Backfill (m^3)	Drain filler (m^3)
16	3449.74–6011.35	33.50–39.03	21.34–113.98	18.08–18.98
14	2418.60–3886.80	27.75–31.01	19.33–103.82	18.01–18.74
12	1790.27–2708.04	21.27–23.38	17.22–93.44	17.14–18.16
10	1387.77–1883.18	16.43–18.91	15.24–83.25	17.04–17.87
8	1007.73–1437.58	13.74–15.34	13.20–72.69	16.61–17.04

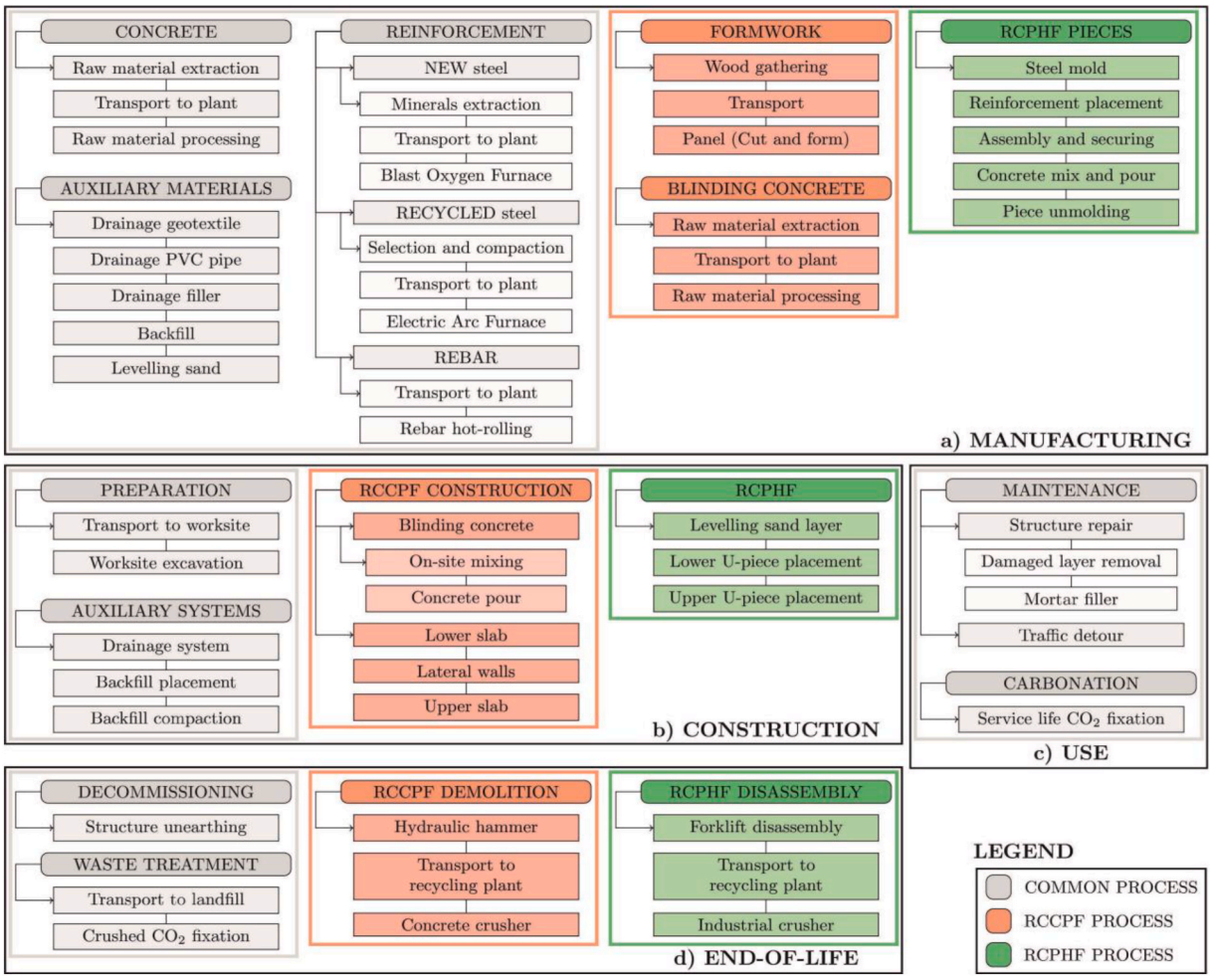

Fig. 2. Life-cycle boundaries applied in the assessment: (a) material production; (b) on-site construction; (c) service and maintenance period; (d) dismantling and recycling phase.

rolling stage, which delivers the rebar used in both frame typologies in proportions consistent with background database averages.

Additional components include geotextile layers, drain fillers, PVC pipes, and backfill material for the surrounding embankments. Typology-specific processes are also modeled: ISRCFs incorporate plywood formwork (with an average reuse of 15 cycles) and 20 MPa blinding concrete, whereas PRCAFs require steel molds for precasting. The impacts associated with mold production and reuse were scaled according to each unit's size following BEDEC guidance (Catalonia Institute of Construction Technology, 2023). Precast manufacturing involves the sequential placement of reinforcement, positioning by cranes, concrete pouring, controlled curing, and demolding after the concrete has hardened (Meireles et al., 2024; Aghasizadeh et al., 2022). Each PRCAF assumes a 45-min crane operation time for handling. The completed elements are stored at the plant before transportation to the site and modeled accordingly within the construction logistics inventory.

2.2.4.2. Construction phase. Construction begins with the on-site delivery of construction materials (ISO, 2006b, 2006c) and excavation of the subgrade to a depth equal to the bottom slab thickness plus 10 cm for levelling.

For ISRCFs, a 10 cm blinding concrete layer is first poured to ensure proper leveling and separation from the foundation soil, thereby providing more uniform contact conditions and improving load transfer between the structure and the subgrade (Sánchez-Garrido et al., 2026b). Reinforcement and formwork for the lower slab are installed, followed by staged casting of walls and top slabs, with adequate curing between pours. In total, three casting stages are required. Timber formwork panels are then removed for reuse. For PRCAFs, assembly is faster: two U-shaped precast elements are positioned over a 10 cm sand layer, using cranes for placement and alignment. Once joined, the system is completed through verification of fit and finish.

Both typologies then share everyday finishing operations, including installing a drainage geotextile along the sidewalls, a PVC pipe embedded in a compacted sand bed, and drain filler near the walls to prevent moisture accumulation. Finally, backfilling and compaction complete the structure's stabilization under equivalent site conditions for both alternatives.

2.2.4.3. Use phase. During the 100-year service life, road frames operate without direct energy demand. Maintenance activities focus on ensuring durability and structural safety, with two scheduled preventive interventions over the lifespan. The diesel consumption for temporary traffic diversions during maintenance is included in the analysis to capture indirect operational impacts. This contribution was modeled using generic transport processes from the Ecoinvent database, representing average European vehicle fleets and fuel consumption patterns. Given the lack of project-specific data (e.g., traffic volume, detour length, or fleet composition), a simplified and consistent assumption was adopted across all configurations. As a result, this contribution should be interpreted as an approximate proxy of indirect operational impacts rather than as a detailed traffic simulation. Since the same assumptions are applied to all alternatives, its influence on the

comparative results remains limited and does not affect the relative differences between structural typologies.

Concrete carbonation occurs progressively throughout the service life. Atmospheric CO_2 reacts with calcium hydroxide, decreasing pH and gradually advancing toward the reinforcement. If carbonation reaches the steel, corrosion may develop; however, the process also enables partial CO_2 sequestration within the concrete matrix. The amount of CO_2 fixed through carbonation is calculated following Fick's first law, as given in Eq. (1) (García-Segura et al., 2014):

$$CO_2(kg) = 0.383 \cdot \frac{k_1\left(\frac{mm}{\sqrt{year}}\right)\cdot\sqrt{t(year)}}{1000}\cdot A\ (m^2)\cdot C\left(\frac{kg}{m^3}\right)\cdot k\ (\%) \quad (1)$$

In this formulation, k_1 represents the carbonation coefficient, t denotes the service life, A the total exposed surface area, C the cement dosage per m^3, and k the proportion of clinker in the binder. Following Lagerblad (2005), a constant value of $k_1 = 1.5$ mm year$^{-0.5}$ was adopted for both internal and external surfaces, consistent with the previously defined concrete composition to ensure comparability across all configurations.

It is acknowledged that carbonation rates may differ between prefabricated and cast-in-place concrete due to variations in curing conditions, compaction levels, and manufacturing processes, which can influence concrete porosity and CO_2 diffusion. However, a uniform carbonation coefficient was adopted to maintain a consistent modeling framework and enable a robust comparative assessment between structural typologies. Given that the primary objective of the study is to evaluate relative differences across design alternatives, this assumption avoids introducing additional variability unrelated to geometric and structural parameters. Furthermore, the contribution of carbonation to the overall Global Warming Potential (GWP) remains secondary compared to the impacts associated with material production, particularly cement consumption. A preliminary sensitivity consideration suggests that moderate variations in the carbonation coefficient would not significantly alter the comparative results between alternatives, as the contribution of carbonation to total GWP remains secondary relative to material production impacts. Future research could refine this aspect by incorporating differentiated carbonation coefficients or performing sensitivity analyses to account for variability in material properties and exposure conditions.

2.2.4.4. End-of-life phase. After completing their 100-year service period, both ISRCF and PRCAF structures are decommissioned through excavation, material separation, and final processing.

For ISRCF, dismantling involves excavation followed by mechanical demolition using a hydraulic hammer, operating at an estimated rate of 20 min per cubic meter of concrete. Reinforcing steel is recovered through magnetic separation and directed to recycling. At the same time, the concrete rubble is transported to a landfill, where full carbonation of the crushed material is assumed, resulting in additional CO_2 uptake consistent with the system boundary defined in Fig. 2.

For precast hinged frames (PRCAF), the modular design allows a more controlled and efficient disassembly process (Ansah et al., 2021). After excavation, the two prefabricated units are lifted using cranes, conveyed to recycling plants, and crushed to separate concrete and steel components. The steel fraction is entirely recycled, and complete carbonation of the concrete residue is again assumed under landfill conditions. Although reuse of precast components in secondary applications has been proposed in prior research, it is not included within the defined scope of this study to maintain consistency between typologies and focus on comparative assessment rather than circularity scenarios.

2.3. Impact analysis approach

The impact evaluation stage translates the quantified outputs obtained from the life-cycle inventory into measurable indicators that reflect the potential environmental and social burdens of the system under comparative assessment conditions. This conversion, performed through life-cycle impact assessment (LCIA) procedures, establishes connections between material flows, energy use, and labor inputs and their corresponding impact categories. Because characterization models and assumptions vary across LCIA methodologies, the selected framework has a decisive influence on how system performance is interpreted when evaluating competing infrastructure alternatives.

To ensure methodological consistency, distinct LCIA models were applied to the environmental and social analyses. The environmental evaluation employed the ReCiPe 2016 methodology (Huijbregts et al., 2017), which combines midpoint and endpoint impact assessment perspectives within a unified LCIA framework. The midpoint perspective provides detailed outputs for multiple environmental categories, each expressed in its native physical units. In contrast, the endpoint model aggregates them into three global areas of impact—human health (DALY), ecosystem integrity (species·year), and depletion of resources (USD). The hierarchical (H) view from the ReCiPe normalization set (H/A, person-year) was used to derive composite impact points, ensuring consistency and comparability between the two structural alternatives within a unified damage-oriented perspective.

In the ReCiPe framework, midpoint results are first characterized in their respective physical units and subsequently translated into endpoint damage categories through established environmental cause–effect pathways. These endpoint indicators are then normalized against reference annual environmental loads associated with the selected hierarchical perspective and weighted to derive the aggregated single-score indicator expressed in impact points. This procedure facilitates comparative interpretation between structural alternatives while preserving methodological consistency across all evaluated configurations.

Although both LCA and S-LCA apply aggregation procedures to facilitate interpretation, the underlying meaning of weighting differs between the two approaches. In ReCiPe, midpoint indicators are aggregated through environmental damage pathways linked to scientifically modeled cause–effect mechanisms. In contrast, the PSILCA/SOCA framework aggregates heterogeneous social risk indicators into stakeholder-oriented medium-risk-hour (MRH) metrics based on predefined risk-weighting structures rather than direct physical damage relationships. Consequently, environmental endpoint results represent damage-oriented impact estimates, whereas social endpoint results should be interpreted as comparative indicators of potential social risk exposure within the adopted database structure.

Employing both midpoint and endpoint representations allows the analysis to capture detailed category-level variations as well as overall sustainability trends. Although the midpoint assessment covers 18 distinct indicators, this study emphasizes Global Warming Potential (GWP) as a benchmark metric, given its central relevance to concrete-based infrastructure and its prominence in infrastructure impact assessment practice. The endpoint analysis, on the other hand, integrates long-term damage results to identify dominant life-cycle stages and determine whether the cast-in-place (ISRCF) or precast (PRCAF) typology achieves better overall environmental outcomes at the system level.

In order to ensure the robustness and statistical consistency of the environmental results, a Monte Carlo–based uncertainty analysis was performed using 1000 simulation runs. This probabilistic approach allowed the statistical characterization of midpoint and endpoint indicators, supporting comparative interpretation across configurations. For the midpoint analysis, representative configurations were selected based on two bounding cases (8 m span with 1 m cover and 16 m span with 5 m cover), capturing the minimum and maximum structural demand conditions within the design space.

The social life-cycle assessment (S-LCA) followed a comparable logic, applying the Social Impacts Weighting Method together with the SOCA v2 database. This dataset aggregates a set of 55 midpoint social

indicators distributed across four stakeholder categories (workers, local community, society, and value chain actors), as defined within the PSILCA framework, which are converted into endpoint metrics expressed in medium-risk hours (MRH). These scores capture the potential cumulative social implications for four groups of stakeholders: employees, supply-chain actors, society, and local residents. For the social assessment, endpoint results were obtained directly from the Social Impact Weighting Method and expressed as absolute medium-risk hour values, enabling consistent comparison across stakeholder categories within a screening-level framework.

The selection of the Social Impacts Weighting Method, the use of medium-risk hours (MRH) as the endpoint metric, and the underlying set of 55 midpoint indicators are consistent with the standardized structure of the PSILCA/SOCA v2 framework, which is widely applied in screening-level social life-cycle assessments. This approach enables the translation of heterogeneous social risk indicators into a common unit (MRH), facilitating comparability across processes, stakeholder categories, and system configurations.

The adoption of this method is aligned with the objective of this study, which focuses on the comparative evaluation of multiple optimized design alternatives under consistent system boundaries. Alternative S-LCA approaches, including those based on site-specific data collection or different activity variables (e.g., working hours or value added), may provide higher resolution for project-level assessments but require detailed primary data that are not available at early design stages. In this context, the use of PSILCA-based activity variables ensures consistency with the life-cycle inventory structure derived from environmental modeling, enabling a coherent integration of environmental and social dimensions. In the SOCA implementation used in this study, the aggregation from midpoint indicators to stakeholder-level endpoint results is performed through the predefined Social Impact Weighting Method embedded within the platform, following the stakeholder-oriented weighting structure provided by the SOCA/PSILCA framework. Accordingly, the reported endpoint MRH values do not represent a direct summation of heterogeneous midpoint risks (e.g., child labor and fair salary), but rather the outcome of a standardized characterization, weighting, and aggregation procedure implemented within the SOCA framework. The present study does not propose a new aggregation methodology and therefore adopts the aggregation logic predefined within the SOCA implementation, interpreting these endpoint values exclusively as comparative screening-level indicators of potential social risk exposure across alternatives.

It is acknowledged that the choice of activity variable and weighting structure may influence the absolute magnitude of social impact results. However, as all alternatives are evaluated under the same methodological assumptions, the observed comparative patterns remain internally consistent within the defined modeling framework. A formal sensitivity analysis based on alternative activity variables (e.g., worker hours or value added) was not performed, as this would require reparameterization of the underlying PSILCA/SOCA model and access to alternative inventory structures beyond the scope of the present study. Nevertheless, to evaluate whether the comparative behavior depended primarily on the aggregation of endpoint results, an additional robustness-oriented consistency analysis was conducted by independently examining the four stakeholder endpoint categories across all optimized configurations. The results, presented in Appendix D, indicate that the comparative trends between cast-in-place and prefabricated alternatives are consistently reproduced across stakeholder categories and are not driven exclusively by the aggregation of total MRH values. Although this analysis does not replace a full activity-variable sensitivity assessment, it provides an additional robustness check supporting the stability of the comparative conclusions within the adopted screening-level framework. Future research could further explore the influence of alternative allocation bases, weighting schemes, and activity variables on S-LCA outcomes.

The aggregation of the 55 midpoint indicators into stakeholder-level endpoint results follows the predefined characterization and weighting structure embedded within the Social Impacts Weighting Method and the SOCA/PSILCA framework. Accordingly, the reported MRH values should be interpreted as comparative indicators of potential social risk exposure rather than as direct measurements of actual social conditions at the project or company level. Differences between structural typologies arise from variations in material demand, process distribution, supply-chain structure, and life-cycle stage contributions, which modify the relative exposure to sector- and country-specific social risk profiles represented in the database. Although alternative weighting schemes could influence the absolute magnitude of results, all configurations were evaluated under the same methodological assumptions, ensuring internally consistent comparison across alternatives. Therefore, the observed comparative trends do not imply that one construction system intrinsically provides better working conditions or social outcomes under all circumstances, but rather that the modeled life-cycle configurations are associated with different distributions of potential social risks within the adopted screening-level framework.

Although midpoint-level results are internally computed within the PSILCA framework, they are not reported individually in this study due to the large number of indicators and the comparative scope of the analysis. Instead, the results are presented at the aggregated endpoint level to facilitate interpretation across multiple design configurations. The contribution of individual midpoint indicators was not extracted separately because the objective of the study was comparative system-level evaluation rather than hotspot attribution at the indicator level. To improve transparency and address the aggregation of social indicators, Appendix C provides a structured overview of the midpoint indicators and their relationship to the aggregated endpoint results. The social impact results are based on the aggregation of 55 midpoint indicators defined within the PSILCA/SOCA v2 framework, encompassing a broad range of social dimensions including labor conditions, human rights, societal well-being, and supply-chain-related risks. This comprehensive indicator set supports the consistency of the aggregated endpoint results and suggests that the observed comparative patterns are not dominated by a single social dimension within the adopted aggregation structure.

Such aggregation enables a harmonized comparison of social outcomes between the two construction systems throughout their entire life cycles for screening-level decision-support rather than predictive social risk quantification. In this context, the adopted approach is particularly suited for early-stage design phases, where multiple structural alternatives must be evaluated under limited data availability, supporting informed typology selection through the identification of trends and trade-offs rather than absolute social performance values. However, it should be acknowledged that, unlike environmental indicators, social impact results are inherently subject to higher levels of variability and epistemic uncertainty due to the aggregated and sector-based nature of PSILCA datasets. While the present study adopts a deterministic approach based on average values to ensure consistency and comparability, recent research has highlighted the importance of incorporating uncertainty and sensitivity analyses in sustainability assessments of concrete and structural systems to improve robustness and interpretability (Gao, 2025; Zhang et al., 2026). This aspect is therefore recognized as a limitation and is proposed as a direction for future methodological enhancement.

While the adopted databases and modeling framework ensure methodological consistency, it should be noted that the underlying inventory data primarily reflect European—particularly Spanish—construction conditions. Consequently, the absolute values of environmental and social impacts may vary when extrapolated to other geographical contexts. Differences in cement production technologies (e.g., clinker ratios and fuel mixes), steel manufacturing routes (BOF versus EAF shares), electricity generation mixes, and the energy efficiency of prefabrication processes can significantly influence environmental outcomes. Likewise, variations in labor structures, supply-chain

organization, and regulatory frameworks may affect the distribution and magnitude of social impact indicators derived from PSILCA. Therefore, the results of this study should be interpreted as comparatively robust within similar technological and regional contexts, while their transferability to other regions should consider local adaptations of life-cycle inventory data and construction practices.

Fig. 3 illustrates the integrated framework that combines environmental, social, and economic dimensions, facilitating a holistic assessment of sustainability within cost-optimized reinforced-concrete road frames and the evaluation of construction alternatives. Environmental and social dimensions are assessed in parallel and interpreted through a multi-indicator perspective, allowing the identification of trade-offs between impact categories and supporting decision-making without relying on a single aggregated sustainability metric.

Complete midpoint social impact results for all road frame configurations are provided in the Supplementary Material in spreadsheet format to improve transparency and reproducibility of the SOCA/PSILCA assessment.

2.4. Interpretation

The interpretation phase provides a structured analysis of the results obtained in the previous stages, aligning them with the study's goals and scope. Here, the emphasis lies in identifying which structural typology—ISRCF or PRCAF—shows lower overall environmental and social impacts and in determining which life-cycle phases most significantly influence those results under different geometric conditions.

The evaluation compares both road frame types across all geometric configurations to reveal the trade-offs within the sustainability-oriented assessment framework. The analysis expresses the relative performance differences through a delta (Δ) parameter, which quantifies either the absolute or percentage variation between alternatives. A positive Δ value indicates that the PRCAF demonstrates superior performance compared with the cast-in-place structure for the evaluated indicator. Conversely, a negative Δ value signifies that the ISRCF achieves better results under the same conditions.

This interpretive approach enables a transparent comparison of the environmental and social differences across all configurations, offering practical insights into which construction approach performs best under specific geometric and operational circumstances and supporting evidence-based typology selection at early project stages.

3. Results

3.1. Evaluation of environmental life cycle performance

Results for each level are presented independently, incorporating Monte Carlo simulations (1000 runs) to obtain average impacts and coefficients of variation (CV), ensuring statistically consistent and reproducible outcomes suitable for comparative infrastructure assessment and enabling a direct interpretation of the reliability of differences between alternatives. The explicit inclusion of CV values allows the evaluation of result dispersion and supports the statistical robustness of the observed differences between structural typologies.

3.1.1. Midpoint-level analysis

The evaluation of midpoint indicators requires the selection of representative impact categories that accurately reflect the primary environmental trends. As analyzing all 18 categories across 50 optimized frame designs exceeds the study's scope, two reference configurations—a short-span case of 8 m with 1 m of soil coverage and a long-span case of 16 m buried under 5 m of soil— were chosen as bounding cases capturing the minimum and maximum structural demand envelopes of the full design domain. Table B.1 (Appendix B) presents the mean values and coefficients of variation, while Figure A.1 (Appendix A) displays the normalized results for enhanced comparability.

Global Warming Potential (GWP), measured in kg CO_2-eq, serves as a key reference indicator in environmental performance evaluations (Bennett et al., 2022; Moro et al., 2022) because of its dominance in infrastructure decision-making and regulatory reporting frameworks. Figure A.2 illustrates how GWP varies with increasing soil cover for each span. Across all configurations, PRCAF alternatives consistently record lower GWP values than ISRCF systems (Table B.2). This behavior is primarily driven by differences in material demand and construction processes, as prefabricated solutions typically require more optimized cross-sections and reduced on-site activities, leading to lower cement consumption and associated emissions.

The sensitivity analysis, derived from a comparative evaluation of mean values across span and burial depth increments, indicates that

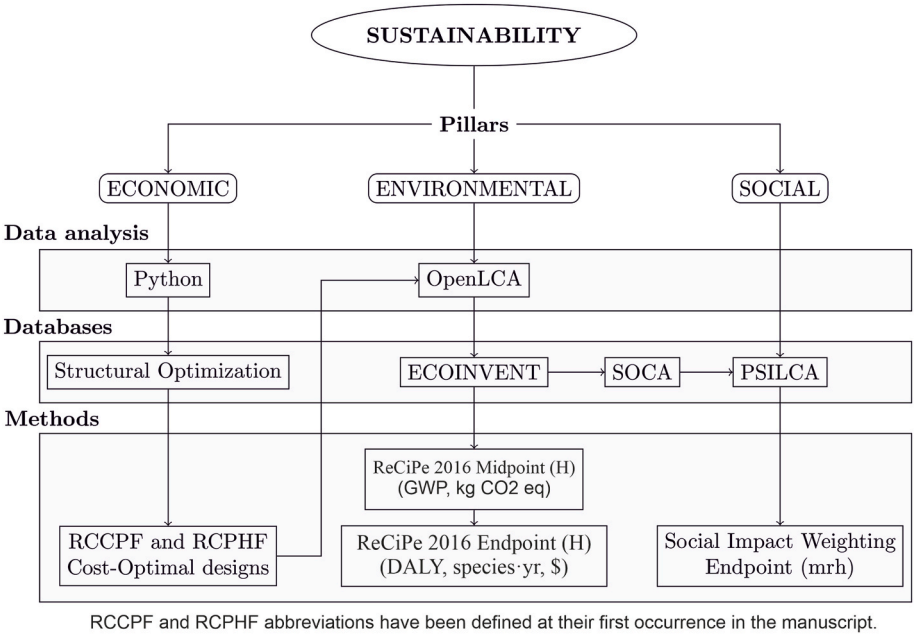

Fig. 3. Framework linking economic optimization with environmental and social life-cycle assessment of reinforced concrete road frames.

span length has a greater influence on GWP than burial depth. Increasing the span by 2 m raises GWP by approximately 23% for ISRCFs and 25% for PRCAFs. In contrast, each additional meter of cover increases GWP by around 11% for both systems. This difference can be explained by the structural response of the frames, as increasing span length requires disproportionately larger cross-sections and reinforcement to satisfy bending and serviceability constraints, thereby significantly increasing material consumption. In contrast, increasing burial depth primarily affects vertical loads, leading to more moderate and approximately linear increases in material demand. The associated coefficients of variation remain below 10% for most configurations, indicating low dispersion and reinforcing the reliability of the observed sensitivity trends with respect to span length and burial depth.

Identifying the most influential life-cycle phases is essential, given the distinct processes of both typologies. Table B.3 and Figure A.4 summarize the mean percentage contributions across burial depths. For ISRCFs, an increase in span shifts contributions toward manufacturing (78% → 88%) due to higher concrete demand. Although maintenance remains constant, carbonation during service reduces the use-phase contribution (4.4% → 1.6%) and enhances end-of-life fixation (−5.8% → −11.3%), concentrating impacts in manufacturing and amplifying the importance of early-stage material efficiency. For PRCAFs, the manufacturing phase becomes increasingly dominant (from approximately 89% up to nearly 100%), owing to the energy-intensive nature of prefabrication, while construction declines (21% → 16%). The use phase slightly decreases (−5.3% → −1.8%), and easier dismantling combined with carbonation improves end-of-life effects (−16.7% → −17.6%). Overall, PRCAFs present lower relative contributions in construction and decommissioning.

Overall, uncertainty levels at the midpoint stage remain moderate, with coefficients of variation generally below 12% for ISRCFs and slightly higher values for PRCAFs due to the increased variability associated with industrialized production processes, and the differences between typologies are generally larger than the observed dispersion levels.

3.1.2. *Endpoint-level analysis*

The endpoint evaluation combines midpoint indicators into three broad categories of damage—ecosystem integrity (species•yr), human health (DALY), and resource use (US$)—providing a concise yet comprehensive picture of the overall performance of the different configurations at the damage-oriented decision-support level. In addition to mean values, the reported coefficients of variation enable a direct assessment of uncertainty at the endpoint level. Across all damage categories, variability remains within acceptable ranges (typically between 7% and 15%), supporting the statistical consistency of the aggregated indicators and indicating that endpoint aggregation does not substantially increase variability relative to midpoint results.

Table B.4 summarizes the results of ecosystem damage, and Fig. 4 illustrates their evolution in terms of span and cover. PRCAFs consistently show lower ecosystem impacts, with an average reduction of 2.25×10^{-5} species·yr (approximately 15.4%). For both structural configurations, ecosystem damage increases quadratically with span length and approximately linearly with burial depth. This behavior reflects the direct relationship between geometric design parameters and material requirements, as longer spans lead to higher concrete volumes and reinforcement ratios, which in turn increase upstream environmental burdens associated with raw material extraction and processing. This trend is consistent with previously reported relationships between geometric parameters and material consumption (Ruiz-Vélez et al., 2023a; Yepes-Bellver et al., 2025). The comparative advantage of PRCAFs decreases as span increases, from approximately 18% at 8 m to about 12% at 16 m. The coefficients of variation reported in Table B.4 indicate moderate dispersion, generally below 13% for PRCAFs and below 10% for ISRCFs, confirming that the observed differences between typologies are robust and not driven by stochastic variability.

For human health damage, the results in Table B.5 and Fig. 5 confirm the same trend: PRCAFs outperform ISRCFs in 24 of 25 configurations, with an average improvement of 9.9% (≈2.6×10^{-3} DALY). The only exception occurs for the 16 m × 5 m configuration, where cast-in-place performs slightly better (approximately 3.8%). Uncertainty levels follow a similar pattern, with coefficients of variation remaining below approximately 11% for most configurations, indicating consistent behavior across the analyzed design space, with differences between alternatives generally exceeding the associated dispersion levels.

The outcomes for resource depletion (Table B.6, Fig. 6) mirror the general performance trend: PRCAFs register reduced resource-related impacts in 23 out of 25 analyzed cases, averaging a 6.5% decrease (approximately 32 USD). This reduction is mainly associated with more efficient use of materials in prefabricated systems, where controlled manufacturing conditions allow better optimization of concrete volumes and reinforcement layouts, reducing the consumption of energy-intensive resources such as cement and steel. Minor exceptions occur for the 12 m and 16 m spans at a burial depth of 5 m, where ISRCFs exhibit slightly better performance. Although the precast typology presents greater variability (with CV values generally around 15–20%, compared to approximately 10–13% for ISRCFs), this higher dispersion remains within typical LCA uncertainty ranges and does not alter the overall comparative trend, as differences between typologies are generally larger than the observed dispersion levels.

The phase contribution analysis (Table B.7, Figure A.5) reveals that manufacturing is the primary contributor to ecosystem damage, with PRCAFs averaging a 7.2% higher contribution than ISRCFs. However, the construction phase consistently contributes less to PRCAFs (≈1.5% lower on average). The end-of-life phase contributes negative values for both typologies due to CO_2 fixation from carbonation, being

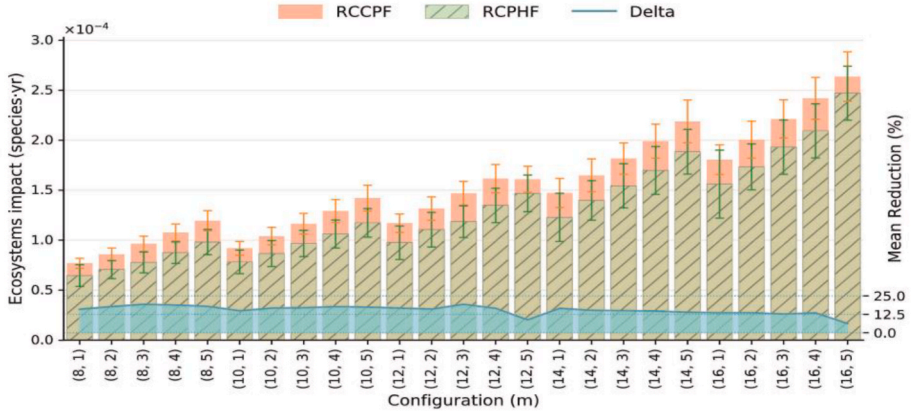

Fig. 4. Ecosystem damage (species·yr) comparison across all design configurations.

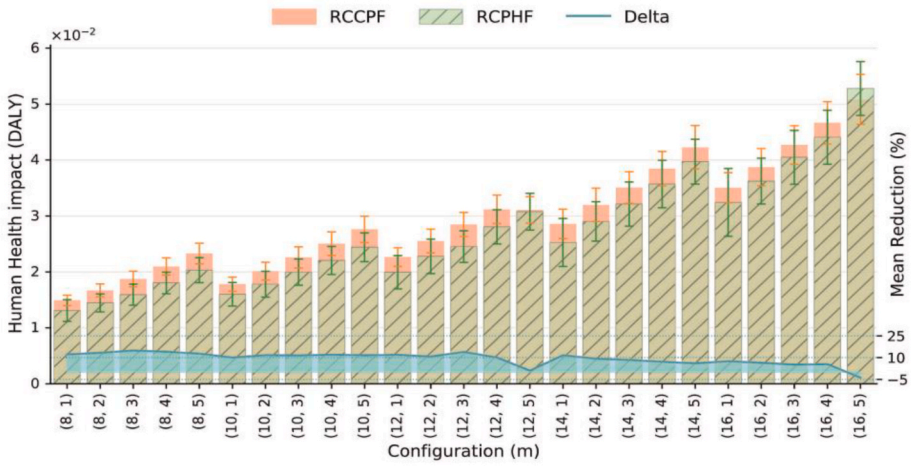

Fig. 5. Human health damage (DALY) comparison among configurations.

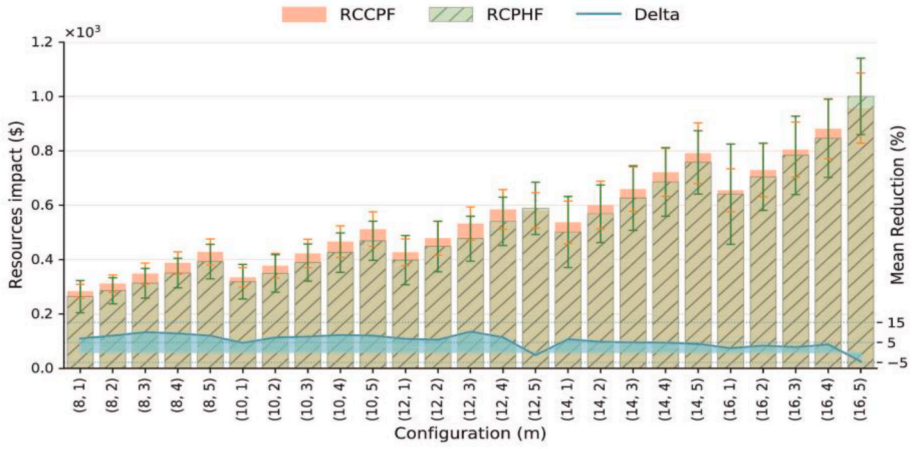

Fig. 6. Resource depletion impact (US$) for each configuration.

approximately 6% lower in PRCAFs.

For human health, Table B.8 and Figure A.6 indicate similar patterns: manufacturing dominates (≈80–90%), while construction impacts are lower for PRCAFs (≈4–5% less). The use and end-of-life phases exhibit more minor but favorable differences, with PRCAFs reducing end-of-life impacts by up to 9.6% relative to ISRCFs.

Regarding resource damage (Table B.9 Figure A.7), the manufacturing phase remains predominant (≈60–75%), especially for PRCAFs. The construction phase impact declines slightly with span due to efficient assembly, while end-of-life contributions diverge—ISRCFs increase from 11% to 13%. In contrast, PRCAFs decrease from 5% to 3.5%.

The relatively low dispersion observed across midpoint and endpoint indicators supports the robustness of the comparative conclusions, particularly regarding the environmental advantage of prefabricated systems across most configurations.

Finally, Table 4 and Fig. 7 present the aggregated single-score results, synthesizing all endpoint categories. The precast typology scores lower in 24 of 25 configurations, confirming its superior overall environmental performance from a damage-weighted multi-criteria perspective. The trends show linear growth with burial depth and quadratic dependence on span, consistent with the structural and material behavior patterns observed in the preceding analyses. This consistency further confirms that aggregated environmental performance is largely governed by material consumption patterns, which are directly controlled by geometric design variables and structural requirements.

Table 4
Overall single-score results for both typologies across all configurations.

Cover (m)	Clear span (m)									
	8.00		10.00		12.00		14.00		16.00	
	ISRCF	**PRCAF**	**ISRCF**	**PRCAF**	**ISRCF**	**PRCAF**	**ISRCF**	**PRCAF**	**ISRCF**	**PRCAF**
5.00	1281.05	1122.33	1528.69	1354.09	1901.50	1695.00	2342.66	2191.04	2825.01	2913.71
4.00	1161.84	1006.15	1392.21	1224.69	1739.88	1550.25	2150.12	1964.96	2604.45	2428.90
3.00	1046.38	888.15	1259.02	1108.62	1582.51	1366.16	1960.11	1772.54	2386.24	2242.47
2.00	933.03	813.96	1128.54	997.46	1425.12	1265.17	1776.30	1605.79	2172.62	2018.33
1.00	840.94	757.72	1001.62	893.73	1270.50	1106.45	1593.33	1410.48	1965.18	1791.40

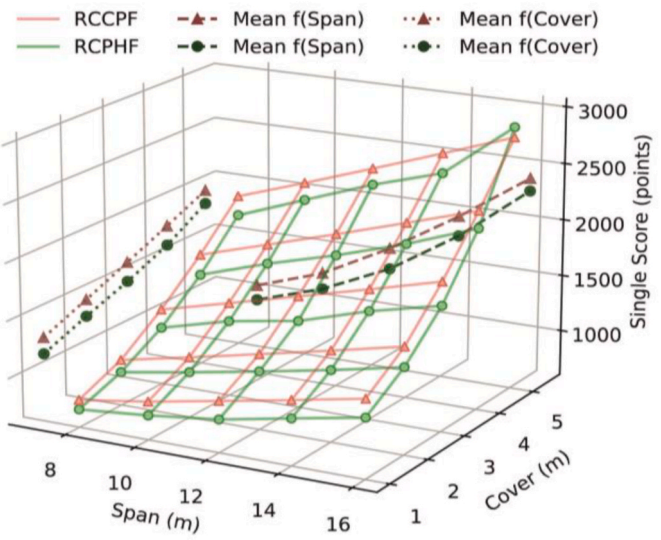

Fig. 7. Aggregated endpoint single-score results for both structural typologies.

3.2. Analysis of social life cycle performance

This section examines social performance across the complete life cycle of the road frame typologies, representing one of the core pillars of sustainability. Table 5 summarizes the endpoint S-LCA results for all cost-optimized configurations, applying a 10^5 normalization factor to present the four aggregated social impact categories—Workers (W), Value Chain Actors (VCA), Society (S), and Local Community (LC)—expressed in medium-risk hours (mrh $\times$ 10^5).

Unlike the environmental assessment, the S-LCA results are not associated with stochastic simulation; therefore, no coefficients of variation are reported. The interpretation is based on deterministic impact values derived from the adopted social database and characterization model. Consequently, the observed differences between typologies should be interpreted as deterministic trends rather than statistically distributed outcomes, although their consistency across configurations supports the robustness of the comparative patterns.

The initial analysis indicates notable differences compared to the environmental outcomes obtained in the E-LCA. As illustrated in Fig. 8, ISRCFs generally exhibit lower social damage, with an average improvement of 4.16 $\times$ 10^5 mrh (2.34%), positioning them as the preferable option from the aggregated S-LCA perspective when impacts are aggregated across all configurations. Both typologies exhibit a quadratic relationship between social damage and span (Fig. 8). For 8–10 m spans, PRCAFs perform better (−3.18 •10^5 mrh, 6.1%), while for 14–16 m spans, ISRCFs dominate (reductions up to 10.8%).

Fig. 9 shows that social damage increases linearly with burial depth, affecting PRCAFs more strongly. PRCAFs outperform ISRCFs only at 1 m cover (−4159 mrh), whereas ISRCFs become superior from 2 m downward, with improvements rising to 8.34 •10^5 mrh (7.7%) at 5 m.

To identify which configuration is most socially sustainable, Fig. 10 details damage differences by stakeholder category. In the Local Community category, PRCAFs outperform ISRCFs for 8 m spans (3.8–9.2% reduction) and maintain small benefits for 10 m spans (1.9%). Beyond 12 m, the advantage alternates with burial depth, disappearing in deeper configurations. For spans of 14–16 m, ISRCFs prevail, with improvements of up to 5 $\times$ 10^5 mrh (≈10%).

Society results follow a comparable trend, with PRCAFs showing 2–9% lower impacts for 8 m spans, whereas ISRCFs outperform them in longer spans, achieving up to 10% lower damage values. In the Value Chain Actors category, PRCAFs remain favorable for short spans (8–10 m) with reductions up to 8.9%, but their advantage fades beyond 12 m, where ISRCFs achieve 4–5% lower damage. For the Workers category, PRCAFs show substantial benefits (up to 18.8%) for spans ≤12 m, while ISRCFs perform better in larger spans, reducing damage by up to 17.6%. Similar trends across stakeholder categories indicate that the comparative behavior is not driven by a single social dimension.

4. Discussion

The results reveal consistent patterns across environmental and social dimensions, while also highlighting important divergences that are strongly dependent on geometric scale and construction approach. These findings provide insight into the mechanisms underlying the observed performance differences and their implications for infrastructure design.

From an environmental perspective, midpoint and endpoint results consistently show that prefabricated systems (PRCAF) achieve lower impacts than cast-in-place alternatives (ISRCF) across most configurations. This advantage is particularly pronounced in Global Warming

Table 5
S-LCA endpoint damage results (mrh·10^5) by stakeholder category for all configurations.

S-categ.		Clear span (m)									
		8.00		10.00		12.00		14.00		16.00	
	Cover	ISRCF	PRCAF	ISRCF	PRCAF	ISRCF	PRCAF	ISRCF	PRCAF	ISRCF	PRCAF
Local Com.	5.00 m	16.30	15.70	19.50	19.30	23.80	25.00	29.70	33.40	36.10	40.00
Local Com.	4.00 m	15.10	14.20	18.10	17.70	22.20	23.10	27.80	30.30	33.90	38.10
Local Com.	3.00 m	13.90	12.70	16.70	16.30	21.20	20.50	25.90	27.50	31.70	35.60
Local Com.	2.00 m	12.70	12.00	15.30	14.90	19.50	19.40	24.60	25.30	29.50	32.40
Local Com.	1.00 m	11.60	11.00	14.00	13.70	17.90	17.30	22.60	22.40	28.00	29.20
Society	5.00 m	17.70	17.40	21.40	21.80	26.90	29.00	34.00	39.70	41.80	48.70
Society	4.00 m	16.60	15.90	20.10	20.20	25.40	27.00	32.20	36.20	39.70	46.10
Society	3.00 m	15.50	14.30	18.80	18.90	24.30	24.10	30.40	33.00	37.60	43.40
Society	2.00 m	14.40	13.80	17.60	17.50	22.80	23.20	29.10	30.70	35.50	39.90
Society	1.00 m	13.40	12.90	16.40	16.40	21.30	20.90	27.20	27.50	33.90	36.30
V. Chain Actors	5.00 m	10.80	10.30	13.10	12.90	15.80	17.00	20.00	23.20	24.50	28.20
V. Chain Actors	4.00 m	10.00	9.40	12.20	11.90	14.90	15.80	18.80	21.10	23.20	26.80
V. Chain Actors	3.00 m	9.33	8.45	11.40	11.10	14.60	14.10	17.70	19.20	21.90	25.10
V. Chain Actors	2.00 m	8.62	8.07	10.50	10.20	13.60	13.50	17.30	17.80	20.60	23.10
V. Chain Actors	1.00 m	7.98	7.51	9.71	9.51	12.60	12.10	16.00	15.90	20.00	20.90
Workers	5.00 m	19.20	18.40	23.20	22.80	28.00	29.80	35.10	40.10	42.80	48.50
Workers	4.00 m	17.90	16.70	21.60	21.00	26.20	27.60	33.00	36.50	40.40	46.10
Workers	3.00 m	16.60	15.00	20.10	19.40	25.70	24.50	30.90	33.10	37.90	43.20
Workers	2.00 m	15.20	14.20	18.50	17.90	23.70	23.40	30.10	30.70	35.50	39.50
Workers	1.00 m	14.00	13.20	17.00	16.50	21.80	20.90	27.70	27.30	34.40	35.70

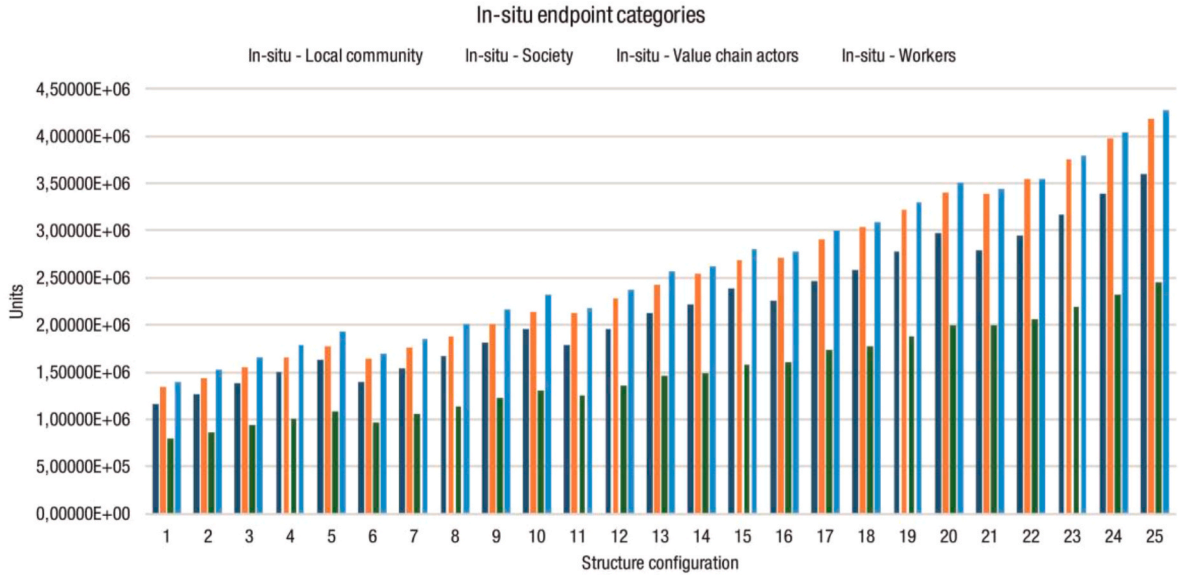

Fig. 8. Evolution of S-LCA endpoint damage with varying horizontal span lengths.

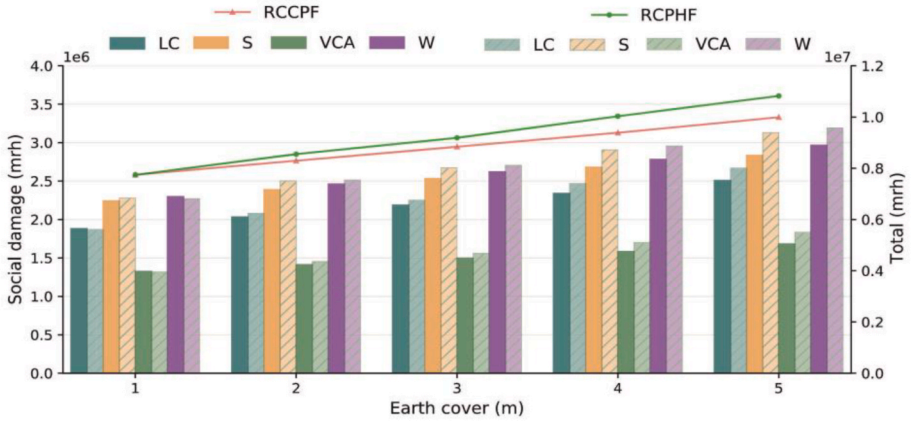

Fig. 9. Variation of S-LCA endpoint damage with increasing soil cover depth.

Potential (GWP), where optimized geometries, reduced material consumption, and carbonation effects contribute to limiting emissions (García-Segura et al., 2014), while improved material efficiency further reduces embodied carbon through lower cement demand and reduced formwork requirements (Bennett et al., 2022). The influence of geometric parameters is also evident, as span length exerts a stronger effect on environmental impacts than burial depth. This behavior is consistent with previous optimization studies on bridges (Yepes-Bellver et al., 2025; Ruiz-Vélez et al., 2023a) and with findings reported by Milić and Bleiziffer (2024), who emphasize the sensitivity of life-cycle results to structural design variables.

At the same time, the environmental advantage of prefabrication is not uniform across all conditions. As span length increases, material intensities between both typologies tend to converge, reducing the relative benefit of PRCAF solutions, even though absolute impact reductions remain significant. This effect is observed across endpoint indicators, including ecosystem damage, human health, and resource depletion. It reflects the increasing dominance of structural demand over construction-related efficiencies in large-scale configurations. Similar patterns have been reported in previous studies, which associate the environmental performance of precast systems with improved material efficiency and reduced on-site activities (Richardson, 2003; Aghasizadeh et al., 2022).

These findings are consistent with previous life-cycle assessment studies on prefabricated and cast-in-place systems in bridges and building structures, which report improved environmental performance of prefabrication due to enhanced material efficiency and reduced on-site activities (Yepes-Bellver et al., 2025; Ruiz-Vélez et al., 2023a; Aghasizadeh et al., 2022). However, the present study extends these insights by demonstrating that such advantages are not constant but depend strongly on geometric scale, with diminishing relative benefits for larger spans. This scale-dependent behavior has been less explicitly addressed in previous studies, which are often based on single or limited design configurations. Furthermore, unlike building and bridge systems, road frame structures exhibit a strong sensitivity to both span length and burial depth, which directly influence structural demand and material consumption patterns. This dual geometric dependency introduces additional complexity in environmental and social life-cycle assessment and contributes to the non-linear trends and trade-offs identified in this study, highlighting the need for parametric and design-oriented evaluation frameworks.

The phase contribution analysis further clarifies these differences. For PRCAF systems, impacts are heavily concentrated in the manufacturing stage due to the energy-intensive nature of prefabrication. In contrast, construction and end-of-life phases contribute less, reflecting simplified assembly processes and more efficient dismantling.

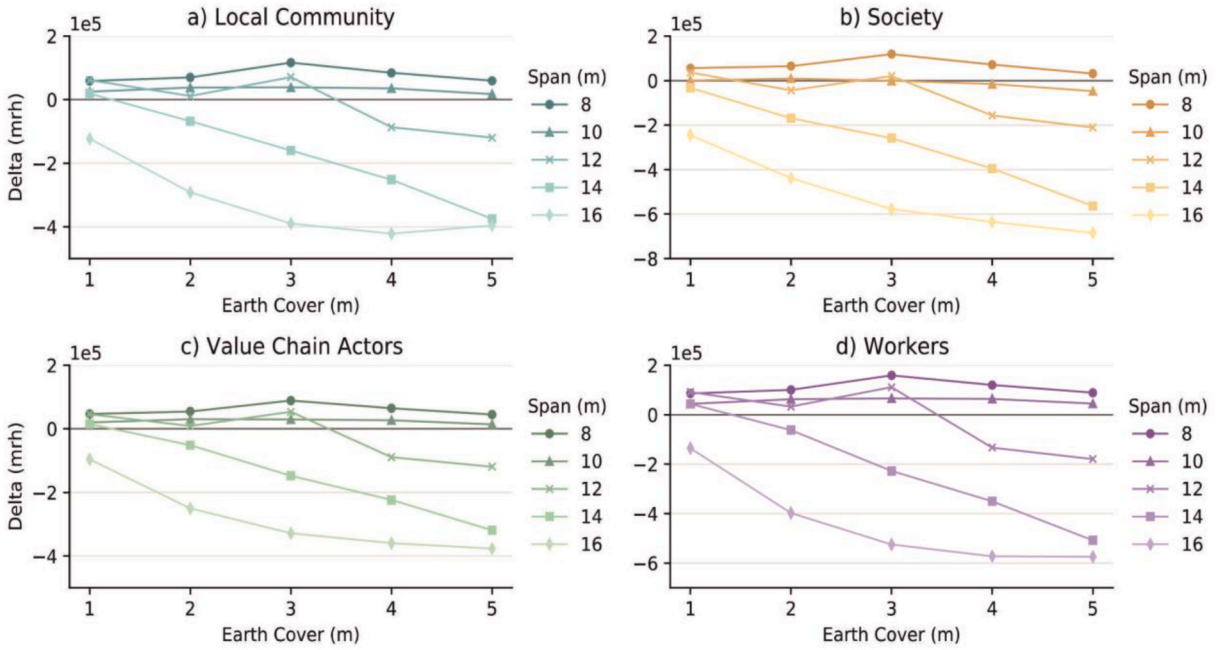

Fig. 10. Comparison of social impact differences between ISRCF and PRCAF by span length, disaggregated by stakeholder group: a) Local Community; b) Society; c) Value Chain Actors; d) Workers.

ISRCF systems exhibit a more distributed impact profile, with relatively higher contributions from construction and end-of-life stages. These differences highlight the importance of early-stage material efficiency and production processes in determining environmental performance, particularly in industrialized construction systems.

In contrast to environmental results, the social assessment reveals a more complex and, in some cases, opposing trend. While prefabricated systems perform better for smaller spans and shallow burial depths, cast-in-place solutions tend to exhibit lower social impacts in larger configurations. This divergence between environmental and social outcomes aligns with previous S-LCA findings for infrastructure systems, where increased labor intensity and a greater relative contribution of localized construction activities within the life cycle can offset the environmental advantages of industrialized construction. It should be noted that these trends are derived from mean S-LCA values within a screening-level framework and are therefore subject to inherent uncertainty associated with aggregated social risk indicators; nevertheless, the consistency of the observed patterns across configurations supports the robustness of the comparative conclusions, in line with recent studies emphasizing uncertainty-aware sustainability assessment in structural systems (Gao, 2025; Zhang et al., 2026).

Moreover, the consistency of these trends across 50 independent optimized configurations suggests that the observed patterns are not dominated by isolated configuration-specific effects within the adopted social-impact framework, providing an additional level of consistency within the screening-level framework. In this context, the observed reversals in relative performance between typologies should be interpreted as deterministic trend-based crossover points rather than statistically significant thresholds, as no stochastic uncertainty propagation is applied in the S-LCA model. The observed trends emerge from the aggregation of multiple social dimensions within the PSILCA framework, including labor conditions, societal factors, and supply-chain-related risks, rather than from isolated indicators.

An additional consistency analysis was conducted at the stakeholder-category level to evaluate whether the observed comparative trends depended primarily on the aggregation of total MRH values. The results, presented in Appendix D, show that the comparative behavior between cast-in-place and prefabricated typologies is independently reproduced across the four stakeholder endpoint categories (workers, local community, society, and value chain actors). This consistency indicates that the identified trends are not generated exclusively by the aggregation procedure or by a single stakeholder dimension, but rather emerge from broader differences in life-cycle process distribution and material demand within the PSILCA/SOCA framework.

This apparent lack of scalability in social benefits contrasts with the environmental advantages of industrialization. While prefabrication benefits from economies of scale in terms of material efficiency and process optimization, these gains do not directly translate into lower social impacts within the S-LCA framework. Social indicators are strongly influenced by the distribution of labor across sectors and regions, as captured by PSILCA-based datasets. As geometric scale increases, the growth in material demand amplifies upstream supply-chain activities associated with manufacturing and raw material extraction, which carry higher social risk intensities. In contrast, cast-in-place systems rely more heavily on localized construction processes, where social risk contributions are distributed differently across stakeholder categories. As a result, the increasing dominance of supply-chain-related impacts at larger scales explains why the relative social advantage of prefabrication diminishes and may reverse for longer spans (Navarro et al., 2024; Sánchez-Garrido et al., 2026a). This behavior is also influenced by the structure of PSILCA-based datasets, where upstream industrial activities tend to concentrate higher social risk intensities than localized construction processes.

A lifecycle-stage perspective helps to further interpret this behavior. In prefabricated systems, social impacts are primarily associated with upstream manufacturing and supply-chain activities, where material production and industrial processes dominate and are linked to higher cumulative social risk exposure in globalized value chains. As geometric scale increases, the growth in material demand further amplifies these upstream contributions. In contrast, cast-in-place systems rely more heavily on construction-stage activities, which are more locally distributed and involve different stakeholder groups, particularly workers and local communities. As a result, while prefabrication reduces impacts in construction phases, it increases the relative importance of upstream stages, whereas cast-in-place systems distribute impacts more evenly across the life cycle. This difference in stage contribution explains

the origin of the observed trade-off between environmental and social performance, particularly for larger spans. Although a quantitative stage-by-stage disaggregation is not available within the aggregated S-LCA framework, the observed trends are consistent with the distribution of material and labor processes across life-cycle stages. These interpretations should be understood as indicative trends derived from the distribution of activities within the PSILCA framework, rather than as direct evidence of specific social conditions at the project level. Because the assessment relies on generic country-sector social risk data rather than project-specific information, the results are intended to support comparative interpretation between alternative structural configurations under consistent modeling assumptions, rather than to predict actual social outcomes for a specific construction project or geographical location. Consequently, the identified trends should be interpreted as relative differences in modeled social risk exposure within the adopted database structure.

For larger spans and deeper burial conditions, cast-in-place systems are associated with lower aggregated social risk exposure, particularly for stakeholder categories related to workers and local communities. This is associated with a higher relative contribution of on-site construction activities within the life cycle, which, in the PSILCA framework, is reflected in the distribution of social risk across stakeholder categories. As a result, traditional construction methods may be associated with lower aggregated social risk exposure for stakeholder categories linked to workers and local communities within the PSILCA framework, particularly in contexts where labor-intensive and locally distributed construction activities represent a larger share of the life cycle.

Overall, the results highlight a clear trade-off between environmental efficiency and social performance. Prefabricated systems tend to minimize environmental impacts through material optimization and process efficiency, whereas cast-in-place systems may be associated with different social impact profiles due to a higher share of labor-intensive and localized construction activities within the life cycle. This trade-off underscores the importance of adopting a multidimensional perspective when evaluating infrastructure alternatives, as single-criterion approaches may overlook critical sustainability factors (Božićek et al., 2021; Bruno et al., 2025).

From a practical standpoint, these findings provide direct guidance for infrastructure decision-making in early design stages. In particular, prefabricated systems (PRCAF) are preferable in scenarios where environmental performance is prioritized, especially for small-to-medium spans and moderate burial depths, where their advantages are more pronounced. Conversely, cast-in-place solutions (ISRCF) may be more suitable in projects where social criteria, such as the relative importance of labor-intensive activities and stakeholder-related social risk exposure, are critical, particularly in large-span configurations. Therefore, the proposed framework enables decision-makers to balance environmental and social objectives by selecting the most appropriate structural typology according to project-specific priorities, regulatory requirements, and local socioeconomic conditions. In this sense, the results are not intended to prescribe a universally optimal solution, but rather to provide structured evidence that supports informed decision-making under competing objectives.

Finally, the observed trends also have implications for the transferability of results. While the general relationships between geometry, material consumption, and life-cycle impacts are consistent with previous literature, the magnitudes of environmental and social impacts may vary across regions, depending on factors such as energy mix, supply chain structure, and labor conditions. This geographical dependency is particularly relevant in S-LCA, where social indicators are linked to country- and sector-specific risk profiles that may vary substantially across regions and supply chains. Consequently, while the absolute magnitude of social impacts may not be directly transferable to different contexts, the study aims primarily to evaluate relative differences between structural alternatives under a harmonized modeling framework. Accordingly, the objective of the present S-LCA is not to predict site-specific social conditions, but rather to identify how alternative structural configurations modify the distribution of potential social risk exposure within a consistent life-cycle modeling structure.

Therefore, the conclusions should be interpreted as representative of the context under study. However, the comparative trends identified (e.g., the relative influence of span length and the trade-offs between prefabrication and cast-in-place solutions) are broadly applicable. Furthermore, the methodological framework itself remains transferable to other regions and construction scenarios, provided that input data are adapted to local conditions. This enables decision-makers to replicate the analysis and obtain context-specific results while preserving the robustness of the comparative insights presented in this study. It should be clarified that, within the proposed framework, economic considerations are incorporated at the design stage through cost optimization, which defines the feasible set of structural configurations, rather than through a full life-cycle costing assessment. In this context, the integration of LCC analysis represents a natural extension of the proposed framework for future research.

It should be noted that the social life-cycle results are derived from a screening-level framework using aggregated PSILCA-based indicators, and therefore carry inherent uncertainty. Despite this, the observed trends across 50 optimized configurations are consistent, supporting the robustness of comparative insights. Future work could incorporate probabilistic and sensitivity analyses for S-LCA to further quantify uncertainties and strengthen evidence-based decision-making in infrastructure planning.

5. Conclusions

This study conducted an extensive life-cycle sustainability analysis comparing two significant types of reinforced concrete road frames: ISRCF and PRCAF, by merging E-LCA and S-LCA approaches within an optimization-based design framework. The assessment of 50 optimized alternatives, varying in span length and soil cover, revealed systematic and geometry-dependent correlations between geometry and sustainability indicators, offering practical guidance for the comparative evaluation of construction alternatives in road infrastructure projects.

The study confirms that geometry is a primary determinant of life-cycle performance. Quantitatively, environmental results show that increasing span length by 2 m leads to impact increases of approximately 23–25% in GWP, whereas each additional meter of burial depth results in an increase of around 11%. Both environmental and social assessments indicate a quadratic dependence of impacts on span length and a linear correlation with burial depth, particularly influencing precast configurations beyond 12 m. These geometric dependencies underscore the necessity of incorporating sustainability criteria into early-stage typology selection and preliminary design, rather than treating them as post-design evaluations.

Precast systems generally show better environmental performance, particularly in embodied emissions. Across the evaluated configurations, PRCAFs achieve lower environmental impacts in the majority of cases, with reductions of approximately 15.4% in ecosystem damage, 9.9% in human health damage, and 6.5% in resource depletion on average. Global Warming Potential (GWP) is lower for spans of 8–10 m, with consistent reductions observed across all burial depths. For larger spans, absolute savings increase but the relative advantage decreases. Cast-in-place systems become comparatively more competitive as span increases, partly due to differences in manufacturing and logistics-related impacts. Phase analysis shows that precast impacts are concentrated in manufacturing, while cast-in-place systems have higher construction and end-of-life impacts. Therefore, prefabrication is advantageous under specific geometric and logistical conditions rather than universally.

Social results, in contrast, depict a more complex and configuration-dependent scenario. PRCAFs outperform in smaller and medium spans

($\leq$12 m), with improvements of up to 18.8% in the Workers category and up to 8.9% for Value Chain Actors, suggesting social benefits linked to improved safety, mechanization, and controlled labor conditions in prefabrication environments. For larger spans ($\geq$14 m), ISRCFs become more socially favorable, with reductions of up to 17.6% in total social damage and improvements reaching approximately 10% depending on the stakeholder category, driven by higher local employment and skill engagement during on-site execution. These findings confirm that environmental and social sustainability may diverge, reinforcing the importance of an integrated approach to capture multidimensional effects in infrastructure planning contexts.

Overall, this research enhances our understanding of how geometric and design parameters influence the environmental and social performance of civil infrastructure. The results indicate that prefabricated systems outperform cast-in-place solutions in 24 out of 25 configurations at the aggregated environmental level, whereas the opposite trend is observed in social performance for larger spans and deeper burial conditions. Through the integration of optimization-driven design with combined environmental and social life-cycle assessment, it proposes a replicable and transferable comparative assessment framework to support evidence-based typology selection in road infrastructure systems. The findings reveal that no single construction method consistently outperforms the other—environmental and social outcomes vary depending on span length, soil cover, and the dominant life-cycle stages involved. Furthermore, although the present study is based on conventional material classes (C25 concrete and B500S steel), the proposed framework is inherently flexible and can be extended to evaluate alternative material grades and more sustainable solutions. By updating the material properties in the structural optimization stage and the corresponding datasets in the life-cycle inventory, the methodology can support the assessment of low-carbon concretes, alternative binders, or recycled materials, enabling its application to emerging sustainability-oriented design strategies.

This study is subject to several limitations that should be acknowledged. The environmental assessment is based on the ReCiPe 2016 method and specific life-cycle inventory assumptions, which may influence the magnitude of certain impact categories, although not the comparative trends observed. This is particularly relevant in a parametric framework, where maintaining a consistent impact assessment method across all alternatives is essential to ensure the robustness of relative comparisons. While uncertainty has been addressed through Monte Carlo simulation, the results remain dependent on the quality and representativeness of input data. In addition, the social assessment relies on a screening-level approach using the Social Impact Weighting Method, providing relative indicators of social risk rather than site-specific evaluations. Furthermore, the analysis is limited to a predefined set of geometric configurations and is primarily based on European (Spanish) construction conditions; therefore, regional differences in cement production, steel supply chains, energy mixes, prefabrication processes, and labor structures may influence the absolute magnitude and distribution of impacts. Consequently, absolute impact magnitudes may vary across regions, although the comparative trends and methodological framework remain transferable.

Future research should build upon this framework by incorporating additional sustainability dimensions, particularly economic assessment, to enable full life-cycle cost–benefit comparisons. Although the present study incorporates cost optimization at the design stage, a full life-cycle cost (LCC) analysis was not explicitly included, as it would require additional assumptions regarding discount rates, maintenance strategies, and economic boundary conditions beyond the scope of this work. Nevertheless, the proposed framework is inherently compatible with LCC methodologies and can be readily extended to integrate economic indicators within the same parametric and optimization-based structure. This would enable a fully integrated sustainability assessment while preserving the parametric and comparative structure proposed in this study. Moreover, the use of region-specific environmental and social datasets would improve the representativeness of results. At the same time, more detailed, site-specific S-LCA approaches could provide deeper insights into stakeholder-level impacts. Extending the methodology to other infrastructure typologies and integrating dynamic or scenario-based analyses would further enhance its applicability within environmental impact assessment processes and strategic infrastructure planning, thereby fostering designs aligned with circularity, social equity, and long-term environmental responsibility. Future developments integrating region-specific datasets, probabilistic S-LCA approaches, and full life-cycle costing methodologies could further enhance decision-support capabilities for sustainable infrastructure planning.

CRediT authorship contribution statement

Andrés Ruiz-Vélez: Conceptualization, Data curation, Formal analysis, Investigation, Methodology, Resources, Software. **Antonio J. Sánchez-Garrido:** Conceptualization, Methodology, Supervision, Validation, Visualization, Writing – original draft, Writing – review & editing. **Julián Alcalá:** Supervision, Validation. **Víctor Yepes:** Funding acquisition, Supervision, Validation, Writing – review & editing.

Declaration of competing interest

The authors whose names are listed immediately below certify that they have NO affiliations with or involvement in any organization or entity with any financial interest (such as honoraria; educational grants; participation in speakers' bureaus; membership, employment, consultancies, stock ownership, or other equity interest; and expert testimony or patent-licensing arrangements), or non-financial interest (such as personal or professional relationships, affiliations, knowledge or beliefs) in the subject matter or materials discussed in this manuscript.

Acknowledgments

Grant PID2023-150003OB-I00 funded by MICIU/AEI/10.13039/501100011033 and by "ERDF/EU".

Appendix A. supplementary figures

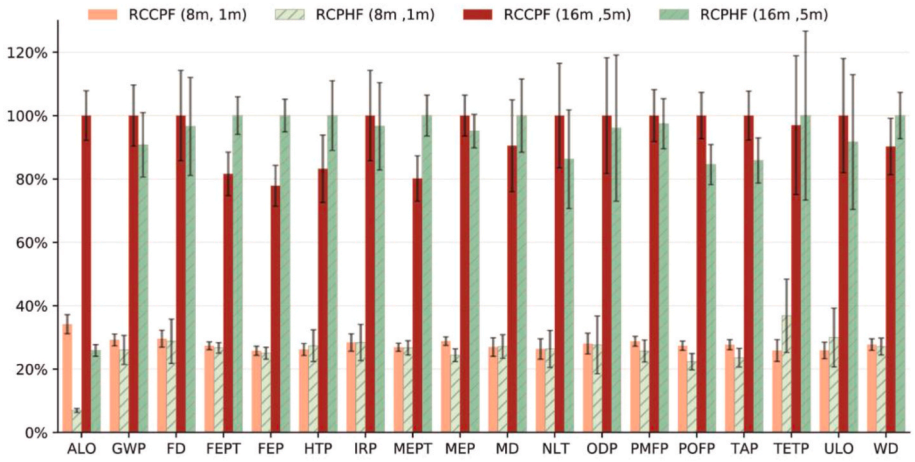

Fig. A.1. Normalized midpoint results for minimum and maximum impact configurations in each typology.

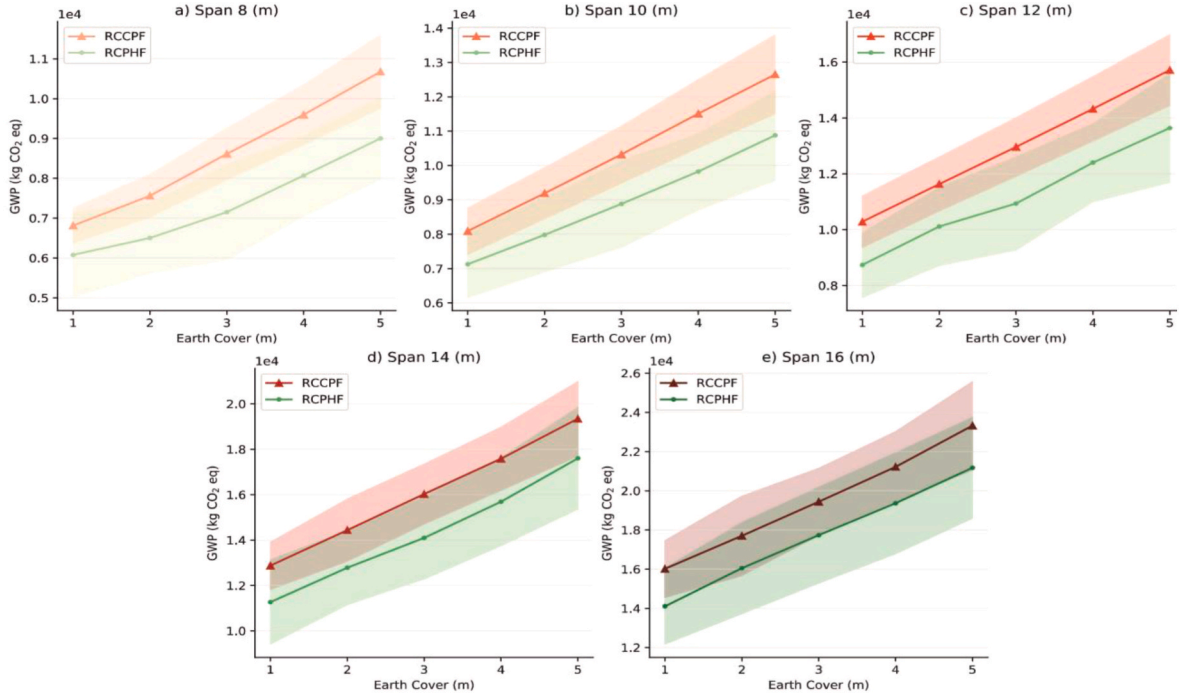

Fig. A.2. Evolution of Global Warming Potential (GWP) with earth cover depth for all spans.

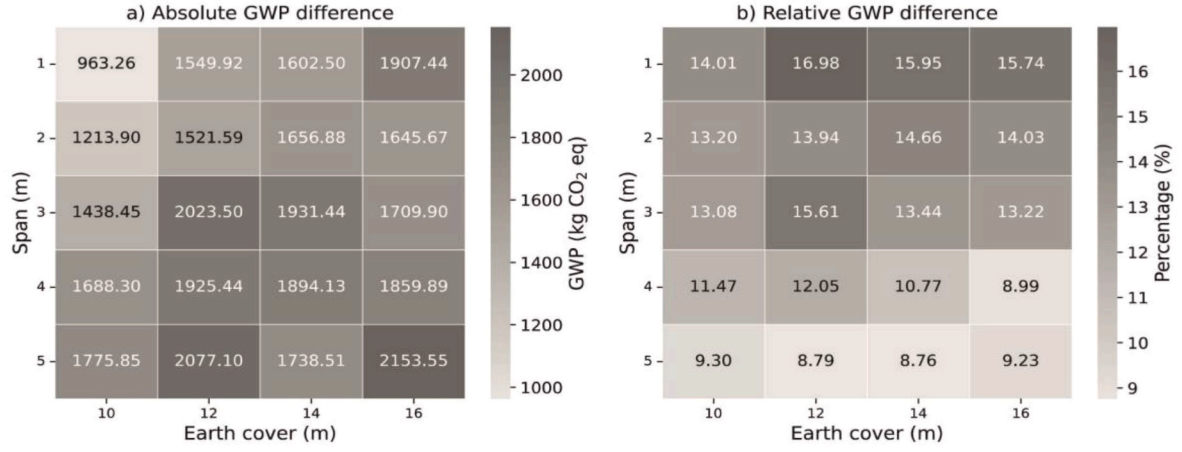

Fig. A.3. Comparative decrease in PRCAF GWP with respect to ISRCF across span and burial depth: (a) absolute variation in GWP; (b) percentage-based differential.

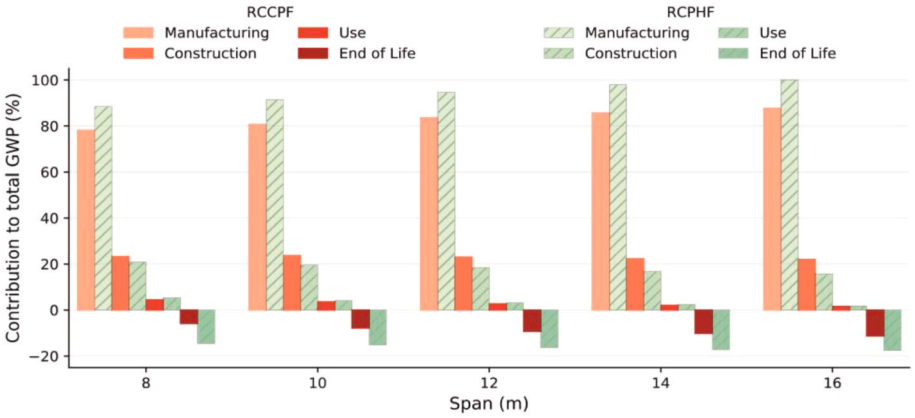

Fig. A.4. Relative impact of individual life-cycle stages on overall GWP for the range of analyzed spans.

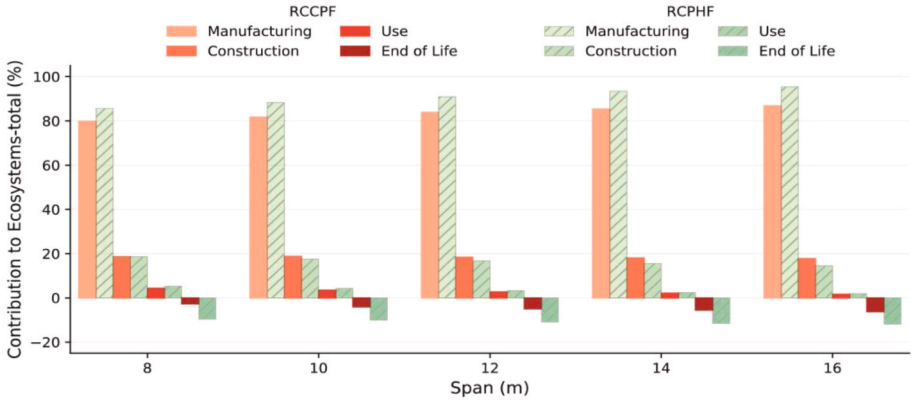

Fig. A.5. Stage-specific share of each life-cycle phase in the overall ecosystem damage (species•yr) across the different span lengths.

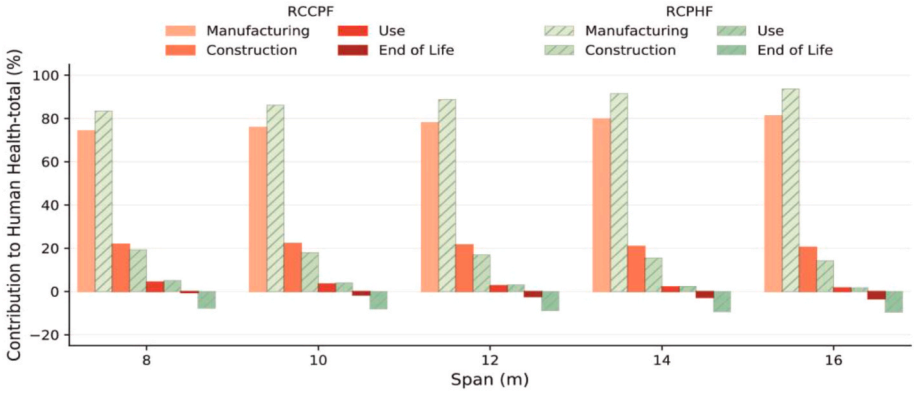

Fig. A.6. Phase contribution to total human health damage (DALY) for varying spans.

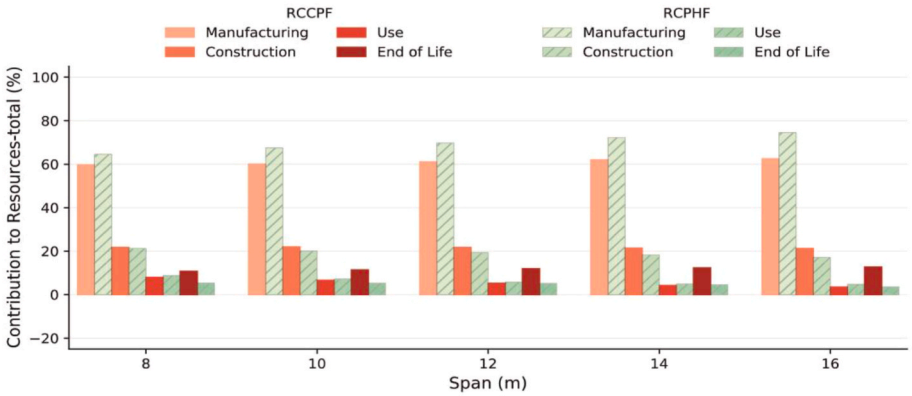

Fig. A.7. Relative contribution of life-cycle phases to resource depletion impacts (US$) by span length.

Appendix B. supplementary tables

Table B.1
Midpoint results corresponding to the least and most impacting configurations for each frame type.

Code			Setup (8.00 m; 1.00 m)				Setup (16.00 m; 5.00 m)			
			ISRCF		PRCAF		ISRCF		PRCAF	
	Environmental Impact	**Measurement**	**Average**	**cv (%)**	**Average**	**cv (%)**	**Average**	**cv (%)**	**Average**	**cv (%)**
WD	Water depletion	m^3	12613.27	6.62	12336.41	9.82	41027.47	9.86	45465.5	7.31
ULO	Urban land occupation	$m^2 \cdot a$	303.56	10.05	351.46	30.94	1172.98	18.03	1075.21	23.22
TEPT	Terrestrial ecotoxicity	kg 1.4-DB eq	0.78	13.28	1.11	31.34	2.93	22.56	3.02	26.66
TAP	Terrestrial acidification	kg SO_2	26.33	5.72	22.42	12.48	95.09	7.72	81.61	8.31
POFP	Photochemical oxidant form.	kg NMVOC	36.74	5.31	29.97	11.57	134.11	7.31	113.39	7.49
PMFP	Particulate matter formation	kg PM10 eq	15.76	5.32	14.08	13.46	54.75	8.18	53.35	8.12
ODP	Ozone depletion	kg CFC-11 eq	6.13E-04	11.72	6.04E-04	32.99	2.19E-03	18.27	1.99E-03	23.99
NLT	Natural land transformation	m^2	2.40	12.23	2.40	22.14	9.10	16.53	7.85	18.05
MD	Metal depletion	kg Fe eq	0.96	10.86	0.97	13.75	3.22	16.04	3.56	11.56
MEP	Marine eutrophication	kg N eq	1.70	4.69	1.44	8.33	5.91	6.46	5.62	5.56
MEPT	Marine ecotoxicity	kg 1.4-DB eq	135.73	4.74	134.76	8.45	404.74	8.92	504.81	6.46
IRP	Ionizing radiation	kg U235 eq	444.12	9.69	444.00	20.15	1563.84	14.28	1511.18	14.26
HTP	Human toxicity	kg 1.4-DB eq	1792.11	7.27	1872.31	18.38	5689.84	12.77	6837.35	11.01
FEP	Freshwater eutrophication	kg P eq	1.77	5.64	1.72	7.48	5.34	8.28	6.86	5.15
FEPT	Freshwater ecotoxicity	kg 1.4-DB eq	144.91	4.53	141.36	6.14	432.17	8.42	529.53	5.93
FD	Fossil depletion	kg oil eq	1711.7	9.01	1664.02	24.37	5783.15	14.29	5585.55	16.02
GWP	Climate change	kg CO_2 eq	6813.6	6.45	6077.43	17.57	23327.56	9.64	21174.01	11.2
ALO	Agricultural land occupation	$m^2 \cdot a$	533.98	8.78	108.52	9.02	1562.59	7.81	404.48	7.14

Table B.2
Global Warming Potential (GWP) values (kg CO_2eq) across all span–cover configurations.

Cover (m)		Clear span (m)									
		8.00		10.00		12.00		14.00		16.00	
	Frame	**Average**	**cv (%)**	**Average**	**cv (%)**	**Average**	**cv (%)**	**Average**	**cv (%)**	**Average**	**cv (%)**
5.00	ISRCF	10680.58	8.64	12656.91	9.08	15716.45	8.03	19343.85	8.49	23327.56	9.64
5.00	PRCAF	8999.63	11.56	10881.06	12.1	13639.35	14.33	17605.34	12.75	21174.01	12.17
4.00	ISRCF	9600.06	7.87	11512.70	8.63	14329.06	8.09	17583.40	7.91	21222.88	8.51
4.00	PRCAF	8068.45	12.71	9824.40	11.46	12403.62	11.37	15689.27	12.39	19362.99	13.32
3.00	ISRCF	8613.37	7.55	10320.37	8.06	12961.39	8.09	16029.49	8.26	19442.74	8.78
3.00	PRCAF	7150.43	16.8	8881.92	14.28	10937.89	15.29	14098.05	12.87	17732.84	13.79
2.00	ISRCF	7562.72	7.15	9193.53	8.07	11634.28	8.31	14442.59	9.48	17704.36	11.43
2.00	PRCAF	6503.24	13.66	7979.63	13.54	10112.69	13.91	12785.71	12.79	16058.69	14.5
1.00	ISRCF	6813.60	6.45	8089.76	8.33	10286.57	9.01	12873.98	8.12	16019.15	9.08
1.00	PRCAF	6077.43	17.57	7126.50	13.58	8736.65	13.33	11271.48	16.48	14111.71	13.75

Table B.3
Average percentage phase contribution to midpoint GWP (kg CO_2eq) by span and typology.

Span (m)	Production phase		Assembly phase		Operation phase		Disposal phase	
	ISRCF	PRCAF	ISRCF	PRCAF	ISRCF	PRCAF	ISRCF	PRCAF
8.00	78.17%	88.52%	23.24%	20.84%	4.43%	5.29%	−5.84%	−14.65%
10.00	80.72%	91.48%	23.61%	19.53%	3.55%	4.15%	−7.87%	−15.16%
12.00	83.62%	94.70%	22.98%	18.49%	2.68%	3.16%	−9.28%	−16.35%
14.00	85.74%	98.03%	22.33%	16.78%	2.04%	2.40%	−10.12%	−17.21%
16.00	87.77%	100.10%	21.95%	15.69%	1.58%	1.76%	−11.31%	−17.55%

Table B.4
Ecosystem damage values (species·yr) × E−04 depending on burial depth and span configuration.

Cover (m)		Clear span (m)									
		8.00		10.00		12.00		14.00		16.00	
	Type	**Average**	**cv (%)**	**Average**	**cv (%)**	**Average**	**cv (%)**	**Average**	**cv (%)**	**Average**	**cv (%)**
5.00	ISRCF	1.20	8.37	1.42	9.03	1.61	8.09	2.19	9.78	2.64	9.39
5.00	PRCAF	0.98	12.83	1.17	12.21	1.47	12.55	1.89	11.89	2.47	10.94
4.00	ISRCF	1.08	7.77	1.29	8.91	1.62	8.72	1.99	8.55	2.42	8.63
4.00	PRCAF	0.87	12.38	1.06	13.16	1.35	12.72	1.70	14.06	2.09	12.93
3.00	ISRCF	0.96	7.93	1.17	8.88	1.47	8.04	1.82	8.61	2.21	8.64
3.00	PRCAF	0.77	13.52	0.96	13.6	1.19	13.37	1.54	14.36	1.93	14.03
2.00	ISRCF	0.85	7.41	1.04	8.38	1.32	8.85	1.65	9.99	2.01	9.18
2.00	PRCAF	0.70	12.77	0.86	14.98	1.11	15.70	1.40	14.16	1.73	13.28
1.00	ISRCF	0.76	6.49	0.92	7.47	1.17	7.83	1.47	9.87	1.81	8.18
1.00	PRCAF	0.64	16.98	0.78	15.09	0.975	17.19	1.23	19.62	1.56	21.78

Table B.5
Human health damage results (DALY) × E−02 according to earth cover and span configuration.

Cover (m)		Clear span (m)									
		8.00		10.00		12.00		14.00		16.00	
	Type	**Average**	**cv (%)**	**Average**	**cv (%)**	**Average**	**cv (%)**	**Average**	**cv (%)**	**Average**	**cv (%)**
5.00	ISRCF	2.33	7.87	2.76	8.53	3.11	7.58	4.23	9.16	5.09	8.80
5.00	PRCAF	2.03	11.01	2.44	10.51	3.08	10.70	3.97	10.06	5.28	9.11
4.00	ISRCF	2.10	7.30	2.51	8.44	3.12	8.18	3.85	8.01	4.67	8.09
4.00	PRCAF	1.80	10.70	2.21	11.33	2.81	10.90	3.57	11.91	4.41	10.93
3.00	ISRCF	1.87	7.48	2.26	8.38	2.85	7.60	3.51	8.05	4.27	8.04
3.00	PRCAF	1.59	11.80	2.00	11.72	2.45	11.50	3.21	12.29	4.05	11.91
2.00	ISRCF	1.67	6.97	2.02	7.90	2.55	8.30	3.20	9.31	3.87	8.57
2.00	PRCAF	1.45	11.17	1.78	12.99	2.28	13.56	2.90	12.14	3.62	11.32
1.00	ISRCF	1.49	6.16	1.78	7.03	2.27	7.38	2.86	9.23	3.51	7.70
1.00	PRCAF	1.31	14.92	1.60	13.15	1.99	14.97	2.53	17.00	3.24	18.66

Table B.6
Resource damage (US$) × E+02 for each combination of span and earth cover depth.

Cover (m)		Clear span (m)									
		8.00		10.00		12.00		14.00		16.00	
	Type	**Average**	**cv (%)**	**Average**	**cv (%)**	**Average**	**cv (%)**	**Average**	**cv (%)**	**Average**	**cv (%)**
5.00	ISRCF	4.29	11.17	5.12	12.50	5.81	11.22	7.91	14.11	9.58	13.50
5.00	PRCAF	3.93	16.15	4.69	15.32	5.89	16.3	7.58	15.37	10.00	14.06
4.00	ISRCF	3.88	10.58	4.66	12.44	5.85	12.46	7.21	12.27	8.82	12.48
4.00	PRCAF	3.51	15.50	4.26	17.03	5.41	16.48	6.86	18.43	8.46	17.01
3.00	ISRCF	3.49	11.19	4.23	12.36	5.33	11.46	6.60	12.38	8.05	12.61
3.00	PRCAF	3.13	17.49	3.89	17.49	4.77	17.34	6.27	18.95	7.84	18.39
2.00	ISRCF	3.12	10.32	3.78	12.00	4.79	12.91	6.01	14.65	7.29	13.49
2.00	PRCAF	2.86	16.77	3.50	19.77	4.49	20.73	5.69	18.64	7.05	17.55
1.00	ISRCF	2.83	9.05	3.35	10.77	4.27	11.43	5.37	14.53	6.55	12.08
1.00	PRCAF	2.64	22.35	3.19	19.94	3.98	22.71	5.02	26.01	6.41	28.74

Table B.7
Average percentage phase contribution to endpoint ecosystem damage (species·yr) by span and typology.

Span (m)	Production phase		Assembly phase		Operation phase			Disposal phase
	ISRCF	PRCAF	ISRCF	PRCAF	ISRCF	PRCAF	ISRCF	PRCAF
8.00	79.83%	85.73%	18.59%	18.60%	4.33%	5.35%	−2.76%	−9.68%
10.00	81.76%	88.35%	18.82%	17.47%	3.52%	4.26%	−4.08%	−10.08%
12.00	83.86%	90.93%	18.43%	16.71%	2.71%	3.30%	−4.97%	−10.94%
14.00	85.40%	93.43%	18.04%	15.63%	2.11%	2.49%	−5.51%	−11.55%
16.00	86.84%	95.44%	17.79%	14.55%	1.67%	1.90%	−6.27%	−11.89%

Table B.8
Average percentage phase contribution to endpoint human health damage (DALY) by span and typology.

Span (m)	Production phase		Assembly phase		Operation phase		Disposal phase	
	ISRCF	PRCAF	ISRCF	PRCAF	ISRCF	PRCAF	ISRCF	PRCAF
8.00	81.26%	93.66%	20.48%	14.21%	1.67%	1.77%	−3.40%	−9.63%
10.00	79.78%	91.50%	20.89%	15.54%	2.11%	2.34%	−2.78%	−9.38%
12.00	78.09%	88.83%	21.55%	16.93%	2.71%	3.10%	−2.35%	−8.86%
14.00	75.88%	86.14%	22.22%	17.95%	3.52%	4.01%	−1.62%	−8.10%
16.00	74.30%	83.44%	21.88%	19.26%	4.34%	5.05%	−0.51%	−7.75%

Table B.9
Average percentage contribution of life-cycle phases to endpoint resource depletion (US$) across both structural systems.

Span (m)	Production phase		Assembly phase		Operation phase		Disposal phase	
	ISRCF	PRCAF	ISRCF	PRCAF	ISRCF	PRCAF	ISRCF	PRCAF
8.00	62.53%	74.56%	21.23%	17.13%	3.47%	4.74%	12.77%	3.58%
10.00	62.05%	72.27%	21.38%	18.26%	4.24%	4.96%	12.33%	4.51%
12.00	61.07%	69.73%	21.70%	19.36%	5.26%	5.80%	11.96%	5.12%
14.00	60.08%	67.52%	21.94%	20.03%	6.62%	7.24%	11.35%	5.20%
16.00	59.63%	64.61%	21.70%	21.29%	7.94%	8.76%	10.73%	5.34%

Appendix C. Midpoint social indicators underlying S-LCA results

This appendix presents the set of midpoint social indicators derived from the PSILCA/SOCA v2 database and used in the assessment. The objective is to illustrate the underlying structure of the aggregated endpoint results (medium-risk hours, MRH) and to provide transparency regarding the range of social dimensions considered in the analysis. The indicators include categories related to labor conditions, supply-chain activities, and societal factors. All 55 midpoint indicators defined within the PSILCA framework are considered in the assessment, ensuring a comprehensive representation of social impacts across the life cycle. Rather than focusing on individual indicators, the S-LCA results are based on their aggregated contribution through the Social Impact Weighting Method. The grouping presented below is intended to facilitate the interpretation of how different social dimensions are reflected in the endpoint results.

Table C.1
Grouping of midpoint social indicators within the PSILCA framework and their contribution to aggregated endpoint results.

Social dimension	Midpoint indicators (PSILCA)	Relation to endpoint results
Labour conditions and workers' rights	Child labour (female, male, total); Forced labour (frequency, goods produced); Fair salary; Weekly working hours; Trade unionism; Violations of employment laws; Gender wage gap; Unemployment; Fatal and non-fatal accidents	Primarily contributes to Workers and Value chain actors
Human rights and societal conditions	Indigenous rights; Corruption (public sector, enterprises); Anti-competitive behaviour; Risk of conflicts; Trafficking in persons	Contributes to Society and Value chain actors
Social well-being and public services	Health expenditure; Expenditures on education; Sanitation coverage; Drinking water coverage; Social security expenditures; Life expectancy; Illiteracy (female, male, total); Youth illiteracy	Primarily contributes to Local community and Society
Supply chain and economic activity	Contribution to economic development; Value added; International migrant workers; Migration flows; Net migration; Sectoral labour force (men/women)	Mainly reflected in Value chain actors and Society
Environmental-social interface	DALYs due to pollution; GHG footprints; Biomass consumption; Fossil fuel consumption; Minerals consumption; Water depletion; Embodied footprints (agricultural, biodiversity, forest, water)	Distributed across all stakeholder categories, especially Society
Governance and social responsibility	Certified environmental management system; Promoting social responsibility; Safety measures	Contributes across all stakeholder categories
Demographic and structural indicators	International migrant stock; Workers affected by natural disasters	Distributed across Society and Local community

Table C.1 summarizes the midpoint social indicators and thematic dimensions included within the PSILCA/SOCA v2 framework and considered in

this study. These indicators are aggregated into endpoint results expressed in medium-risk hours (MRH) through the Social Impact Weighting Method. It should be noted that the relationship between midpoint indicators and endpoint results is not a one-to-one correspondence, but rather the outcome of a weighted aggregation process embedded within the PSILCA methodology. Therefore, the grouping presented in Table C.1 is intended to provide a conceptual interpretation of how different social dimensions contribute to the aggregated results. This presentation is intended to enhance transparency and support the interpretation of aggregated results, rather than to establish a direct causal attribution between individual midpoint indicators and specific endpoint values.

Appendix D. Robustness analysis of stakeholder-category S-LCA results

The S-LCA results presented in this study are primarily discussed using aggregated endpoint values expressed in medium-risk hours (MRH). In order to evaluate whether the observed comparative trends between structural typologies were influenced by the aggregation procedure itself, an additional robustness-oriented consistency analysis was performed at the stakeholder-category level.

The analysis separately examined the four stakeholder endpoint categories defined within the PSILCA/SOCA v2 framework:

- workers,
- local community,
- society,
- and value chain actors.

For each optimized configuration, the endpoint contributions of these categories were independently compared between cast-in-place (ISRCF) and prefabricated (PRCAF) alternatives.

The results indicate that the comparative behavior observed in the aggregated MRH values is consistently reproduced across the different stakeholder categories. In particular, the relative increase in social risk exposure associated with prefabricated solutions at larger spans is not attributable to a single stakeholder group, but reflects a broader shift in the distribution of social risk contributions across multiple stakeholder dimensions.

This consistency suggests that the comparative trends identified in the study are structurally linked to variations in material demand, supply-chain intensity, and life-cycle process distribution within the adopted PSILCA/SOCA framework, rather than being solely generated by endpoint aggregation effects.

It should be noted that this analysis does not constitute a full sensitivity assessment of alternative activity variables or weighting schemes, which would require reparameterization of the underlying S-LCA model. Nevertheless, the independent evaluation of stakeholder endpoint categories provides an additional level of methodological transparency and supports the robustness of the comparative conclusions within the adopted screening-level framework.

While the stakeholder-category analysis does not eliminate the inherent limitations associated with generic PSILCA/SOCA datasets, it indicates that the comparative behavior identified in the aggregated endpoint results is systematically reproduced across multiple social dimensions and stakeholder groups. The figures illustrate the evolution of stakeholder-category endpoint results across span lengths and burial depths for both structural typologies. The consistency of comparative trends across stakeholder categories supports the stability of the aggregated MRH-based interpretation within the adopted PSILCA/SOCA framework.

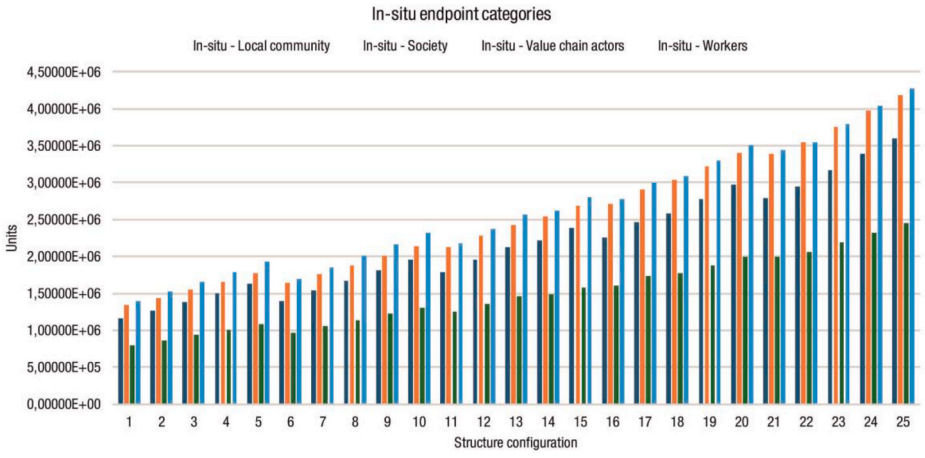

Fig. D.1. Stakeholder endpoint categories for ISRCF configurations.

Table D.1
Stakeholder-category endpoint results for optimized cast-in-place configurations (ISRCF).

Type	Span (m)	Depth (m)	Local community	Society	Value chain actors	Workers	Total
In-Situ	8	1	1.15809E+06	1.34179E+06	7.97822E+05	1.40144E+06	4.69914E+06
	8	2	1.26692E+06	1.44119E+06	8.62237E+05	1.52206E+06	5.09241E+06
	8	3	1.38617E+06	1.54981E+06	9.33440E+05	1.65514E+06	5.52457E+06
	8	4	1.50580E+06	1.65829E+06	1.00478E+06	1.78835E+06	5.95723E+06
	8	5	1.62840E+06	1.76888E+06	1.07767E+06	1.92452E+06	6.39947E+06
	10	1	1.39752E+06	1.63796E+06	9.71363E+05	1.69755E+06	5.70440E+06
	10	2	1.53303E+06	1.76055E+06	1.05351E+06	1.85116E+06	6.19826E+06
	10	3	1.67098E+06	1.88477E+06	1.13691E+06	2.00713E+06	6.69979E+06
	10	4	1.80987E+06	2.00929E+06	1.22074E+06	2.16383E+06	7.20372E+06
	10	5	1.95085E+06	2.13515E+06	1.30564E+06	2.32252E+06	7.71417E+06
	12	1	1.78854E+06	2.12555E+06	1.25715E+06	2.18365E+06	7.35488E+06
	12	2	1.95391E+06	2.27772E+06	1.35941E+06	2.37361E+06	7.96464E+06
	12	3	2.12174E+06	2.43161E+06	1.46297E+06	2.56600E+06	8.58233E+06
	12	4	2.22222E+06	2.53912E+06	1.49070E+06	2.62344E+06	8.87548E+06
	12	5	2.38305E+06	2.68795E+06	1.58462E+06	2.79863E+06	9.45425E+06
	14	1	2.26126E+06	2.71762E+06	1.60419E+06	2.77305E+06	9.35612E+06
	14	2	2.46144E+06	2.90530E+06	1.73029E+06	3.00576E+06	1.01028E+07
	14	3	2.58587E+06	3.04068E+06	1.77116E+06	3.08687E+06	1.04846E+07
	14	4	2.77677E+06	3.22167E+06	1.88425E+06	3.29666E+06	1.11793E+07
	14	5	2.96734E+06	3.40177E+06	1.99705E+06	3.50575E+06	1.18719E+07
	16	1	2.79594E+06	3.38573E+06	1.99574E+06	3.43844E+06	1.16158E+07
	16	2	2.94866E+06	3.55110E+06	2.05515E+06	3.55295E+06	1.21078E+07
	16	3	3.16592E+06	3.76051E+06	2.18516E+06	3.79316E+06	1.29047E+07
	16	4	3.38669E+06	3.97240E+06	2.31698E+06	4.03687E+06	1.37129E+07
	16	5	3.60553E+06	4.18189E+06	2.44761E+06	4.27808E+06	1.45131E+07

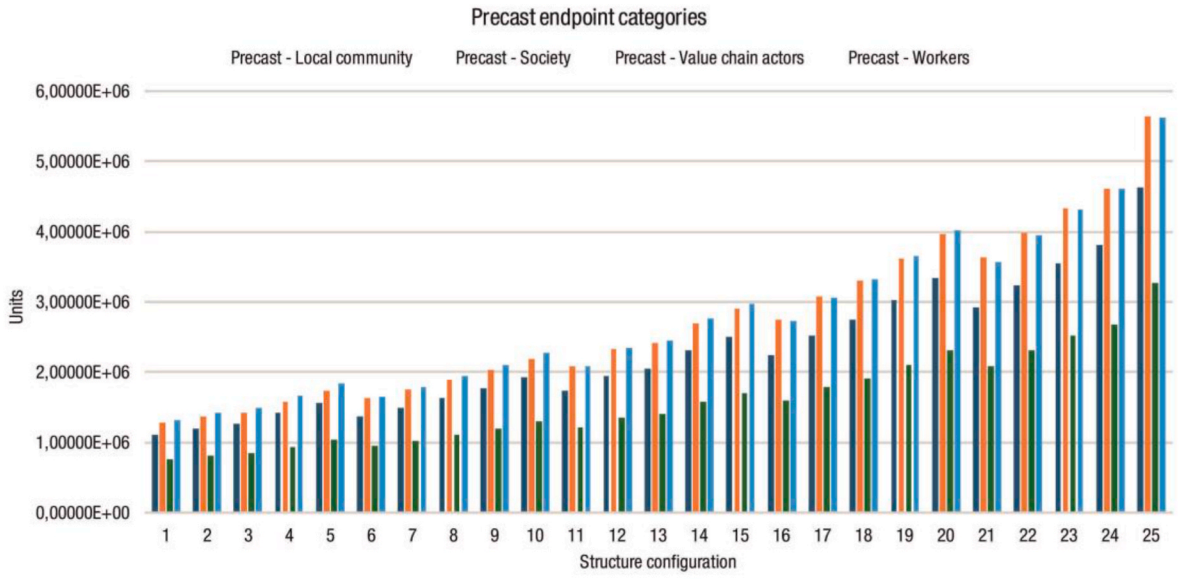

Fig. D.2. Stakeholder endpoint categories for PRCAF configurations.

Table D.2
Stakeholder-category endpoint results for optimized cast-in-place configurations (PRECAST).

Type	Span (m)	Depth (m)	Local community	Society	Value chain actors	Workers	Total
Precast	8	1	1,09947E+06	1,28620E+06	7,50594E+05	1,31522E+06	4,45148E+06
	8	2	1,19672E+06	1,37596E+06	8,07330E+05	1,42154E+06	4,80154E+06
	8	3	1,26978E+06	1,43035E+06	8,44625E+05	1,49604E+06	5,04080E+06
	8	4	1,42148E+06	1,58655E+06	9,40093E+05	1,66834E+06	5,61646E+06
	8	5	1,56898E+06	1,73752E+06	1,03279E+06	1,83552E+06	6,17480E+06
	10	1	1,37240E+06	1,63678E+06	9,51406E+05	1,65353E+06	5,61412E+06
	10	2	1,49478E+06	1,75103E+06	1,02330E+06	1,78779E+06	6,05690E+06
	10	3	1,63232E+06	1,88570E+06	1,10704E+06	1,94128E+06	6,56634E+06
	10	4	1,77440E+06	2,02484E+06	1,19349E+06	2,09978E+06	7,09250E+06
	10	5	1,93316E+06	2,18238E+06	1,29118E+06	2,27763E+06	7,68435E+06
	12	1	1,72732E+06	2,08933E+06	1,21084E+06	2,09196E+06	7,11945E+06
	12	2	1,94274E+06	2,32118E+06	1,35062E+06	2,34089E+06	7,95543E+06

(*continued on next page*)

Table D.2 (*continued*)

Type	Span (m)	Depth (m)	Local community	Society	Value chain actors	Workers	Total
	12	3	2,05074E+06	2,41073E+06	1,40957E+06	2,45480E+06	8,32584E+06
	12	4	2,30879E+06	2,69607E+06	1,58015E+06	2,75601E+06	9,34101E+06
	12	5	2,50277E+06	2,89880E+06	1,70368E+06	2,97768E+06	1,00829E+07
	14	1	2,24160E+06	2,74993E+06	1,58913E+06	2,72933E+06	9,30998E+06
	14	2	2,52910E+06	3,07422E+06	1,78176E+06	3,06770E+06	1,04528E+07
	14	3	2,74556E+06	3,29901E+06	1,91875E+06	3,31442E+06	1,12777E+07
	14	4	3,02844E+06	3,61702E+06	2,10808E+06	3,64693E+06	1,24005E+07
	14	5	3,34235E+06	3,96536E+06	2,31613E+06	4,01369E+06	1,36375E+07
	16	1	2,91874E+06	3,63075E+06	2,09179E+06	3,57327E+06	1,22146E+07
	16	2	3,24039E+06	3,98968E+06	2,30564E+06	3,95011E+06	1,34858E+07
	16	3	3,55543E+06	4,33835E+06	2,51394E+06	4,31800E+06	1,47257E+07
	16	4	3,80828E+06	4,60783E+06	2,67682E+06	4,60914E+06	1,57021E+07
	16	5	4,63471E+06	5,63588E+06	3,27104E+06	5,62057E+06	1,91622E+07

Data availability

Data will be made available on request.

References

Aghasizadeh, S., Tabadkani, A., Hajirasouli, A., Banihashemi, S., 2022. Environmental and economic performance of prefabricated construction: a review. Environ. Impact Assess. Rev. 97, 106897. https://doi.org/10.1016/j.eiar.2022.106897.

Al-Obaidy, M., Courard, L., Attia, S., 2022. A parametric approach to optimizing building construction systems and carbon footprint: a case Study inspired by circularity principles. Sustainability 14 (6), 3370. https://doi.org/10.3390/su14063370.

Almulhim, M.S.M., Logaby, M.J., Bongwirnso, U.M., 2025. Environmental impact assessment of floor system spans: a life cycle approach for sustainable structures. Results Eng., 106851 https://doi.org/10.1016/j.rineng.2025.106851.

Ansah, M.K., Chen, X., Yang, H., Lu, L., Lam, P.T.I., 2021. Developing an automated BIM-based life cycle assessment approach for modularly designed high-rise buildings. Environ. Impact Assess. Rev. 90, 106618. https://doi.org/10.1016/j.eiar.2021.106618.

Ashraf, A.I., Mohareb, E., Vahdati, M., Khandakar, A., 2025. Social life cycle assessment (S-LCA) of formal and informal waste collectors in decentralized waste to compost facility. Clean. Environ. Syst. 17, 100284. https://doi.org/10.1016/j.cesys.2025.100284.

Ayarkwa, J., Joe Opoku, D.-G., Antwi-Afari, P., Li, R.Y.M., 2022. Sustainable building processes' challenges and strategies: the relative important index approach. Clean. Eng. Technol. 7, 100455. https://doi.org/10.1016/j.clet.2022.100455.

Backes, Jana Gerta, Traverso, Marzia, 2024. Social life cycle assessment in the construction industry: systematic literature review and identification of relevant social indicators for carbon reinforced concrete. Environ. Dev. Sustain. 26, 7199–7233. https://doi.org/10.1007/s10668-023-03005-6, 2024.

Barahmand, Z., Wang, L., Eikeland, M., 2026. Mapping the circular economy: insights from 2,701 indicators. Clean. Environ. Syst. 20, 100392. https://doi.org/10.1016/j.cesys.2025.100392.

Barbero, I., Rezgui, Y., Beach, T., et al., 2024. Social life cycle assessment in the construction sector: current work and directions for future research. Int. J. Life Cycle Assess. 29, 1827–1845. https://doi.org/10.1007/s11367-024-02341-7.

Bennett, B., Visintin, P., Xie, T., 2022. Global warming potential of recycled aggregate concrete with supplementary cementitious materials. J. Build. Eng. 52, 104394. https://doi.org/10.1016/j.jobe.2022.104394.

Božićek, D., Kunič, R., Košir, M., 2021. Interpreting environmental impacts in building design: application of a comparative assertion method in the context of the EPD scheme for building products. J. Clean. Prod. 279, 123399. https://doi.org/10.1016/j.jclepro.2020.123399.

Bruno, A., Menichini, T., Silvestri, L., 2025. Life cycle sustainability assessment (LCSA): a comprehensive overview of existing integrated approaches to LCA, S-LCA, and LCC. Eur. J. Sustain. Dev. 14 (3), 13. https://ecsdev.org/ojs/index.php/ejsd/article/view/1743.

Casale, M., Oggeri, C., Rossi, P., Dino, G.A., 2025. Performance assessment of recycled aggregates from C&DW plants for road embankments: influence of composition and treatment methods. Results Eng. 28, 107340. https://doi.org/10.1016/j.rineng.2025.107340.

Catalonia Institute of Construction Technology, 2023. BEDEC ITEC Updated Materials Database from. https://metabase.itec.cat/vide/es/bedec. (Accessed 21 April 2023).

CEN (European Committee for Standardization), 2013. Eurocode 2: Design of Concrete Structures. CEN, Brussels.

Ciroth, A., 2007. ICT for environment in life cycle applications openLCA—A new open source software for life cycle assessment. Int. J. Life Cycle Assess. 12 (4), 209–210. https://doi.org/10.1065/lca2007.06.337.

Ciroth, A., Muller, S., Weidema, B., Lesage, P., 2016. Empirically based uncertainty factors for the pedigree matrix in ecoinvent. Int. J. Life Cycle Assess. 21, 1338–1348. https://doi.org/10.1007/s11367-013-0670-5.

Firoozi, A.A., Firoozi, A.A., Oyejobi, D.O., Avudaiappan, S., Flores, E.S., 2024. Emerging trends in sustainable building materials: technological innovations, enhanced performance, and future directions. Results Eng. 24, 103521. https://doi.org/10.1016/j.rineng.2024.103521.

Frischknecht, R., Rebitzer, G., 2005. The ecoinvent database system: a comprehensive web-based LCA database. J. Clean. Prod. 13 (13), 1337–1343. https://doi.org/10.1016/j.jclepro.2005.05.002.

Gao, S., 2025. Life cycle sustainability assessment of concrete-filled steel tubular frames in earthquake regions. Eng. Struct. 328, 119761. https://doi.org/10.1016/j.engstruct.2025.119761.

Gao, S., Li, W., Yuan, K., Rong, C., 2023. Properties and application of thixotropic cement paste backfill with molybdenum tailings. J. Clean. Prod. 391, 136169. https://doi.org/10.1016/j.jclepro.2023.136169.

Gao, S., Zhao, G., Guo, L., Zhou, L., Yuan, K., 2021. Utilization of coal gangue as coarse aggregates in structural concrete. Constr. Build. Mater. 268, 121212. https://doi.org/10.1016/j.conbuildmat.2020.121212.

García-Segura, T., Yepes, V., Alcalá, J., 2014. Life cycle greenhouse gas emissions of blended cement concrete including carbonation and durability. Int. J. Life Cycle Assess. 19 (1), 3–12. https://doi.org/10.1007/s11367-013-0614-0.

Garcia, A.S., Mendes-Da-Silva, W., Orsato, R.J., 2017. Sensitive industries produce better ESG performance: evidence from emerging markets. J. Clean. Prod. 150, 135–147. https://doi.org/10.1016/j.jclepro.2017.02.174.

Garcia, J., Villavicencio, G., Altimiras, F., Crawford, B., Soto, R., Minatogawa, V., Franco, M., Martínez-Muñoz, D., Yepes, V., 2022. Machine learning techniques applied to construction: a hybrid bibliometric analysis of advances and future directions. Autom. ConStruct. 142, 104532. https://doi.org/10.1016/j.autcon.2022.104532.

GreenDelta, 2013. Greendelta PSILCA v1.0 (Product Social Impact Life-Cycle Assessment). GreenDelta, Berlin, Germany.

Hack, J., Prytula, M., Rieniets, T., Rosenberger, J., 2025. Life cycle assessment for urban planning: a modular approach to integrating buildings and infrastructure. Circ. Econ. Sustain. 5 (6), 5195–5219. https://doi.org/10.1007/s43615-025-00671-8.

Huijbregts, M.A.J., Steinmann, Z.J.N., Elshout, P.M.F., Stam, G., Verones, F., Vieira, M., Zijp, M., Hollander, A., Van Zelm, R., 2017. ReCiPe2016: a harmonised life cycle impact assessment method at midpoint and endpoint level. Int. J. Life Cycle Assess. 22, 138–147. https://doi.org/10.1007/s11367-016-1246-y.

Imbabi, M.S., Carrigan, C., McKenna, S., 2012. Trends and developments in green cement and concrete technology. Int. J. Sustain. Built Environ. 1 (2), 194–216. https://doi.org/10.1016/j.ijsbe.2013.05.001.

International Organization for Standardization (ISO), 2006a. Environmental Labels and Declarations – Type III Environmental Declarations – Principles and Procedures. ISO, Geneva, Switzerland.

International Organization for Standardization (ISO), 2006b. Environmental Management – Life Cycle Assessment – Principles and Framework. ISO, Geneva, Switzerland.

International Organization for Standardization (ISO), 2006c. Environmental Management – Life Cycle Assessment – Requirements and Guidelines. ISO, Geneva, Switzerland.

Kanwal, Q., Xu, G., Gari, Z., Alhusainan, R.S., Al-Ghamdi, S.G., 2025. Attributional life cycle assessment of recycling and disposal strategies for construction and demolition waste. Clean. Environ. Syst. 18, 100283. https://doi.org/10.1016/j.cesys.2025.100283.

Kaveh, A., Bakhshpoori, T., Barkhori, M., 2014. Optimum design of multi-span composite box girder bridges using cuckoo search algorithm. Steel Compos. Struct. 17 (5), 703–717. https://doi.org/10.12989/scs.2014.17.5.703.

Kufner, F., Steinhauer, J., Rucker-Gramm, P., Horstmann, M., 2025. Holistic sustainability assessment of textile-reinforced concrete compared to structural concrete using the example of a roof construction. Clean. Environ. Syst. 19, 100331. https://doi.org/10.1016/j.cesys.2025.100331.

Labaran, Y.H., Mathur, V.S., Muhammad, S.U., Musa, A.A., 2022. Carbon footprint management: a review of construction industry. Clean. Eng. Technol. 9, 100531. https://doi.org/10.1016/j.clet.2022.100531.

Lagerblad, B., 2005. Carbon dioxide uptake during concrete life cycle – state of the art. Swedish Cement and Concrete Research Institute.

Li, H., Zhang, M., AzariJafari, H., Kirchain, R., 2025. Advancing smart and sustainable road construction and maintenance through life-cycle optimisation of concrete pavements. Intelligent Transportation Infrastructure 4. https://doi.org/10.1093/iti/liaf029 liaf029.

Meireles, I., Martín-Gamboa, M., Sousa, V., Kalthoum, A., Dufour, J., 2024. Comparative environmental life cycle assessment of partition walls: innovative prefabricated systems vs conventional construction. Clean. Environ. Syst. 12, 100179. https://doi.org/10.1016/j.cesys.2024.100179.

Milić, I., Bleiziffer, J., 2024. Life cycle assessment of the sustainability of bridges: methodology, literature review and knowledge gaps. Frontiers in Built Environment 10, 1410798. https://doi.org/10.3389/fbuil.2024.1410798.

Ministerio de Fomento (MFOM), 2011. IAP-11: Code on the Actions for the Design of Road Bridges. MFOM, Madrid.

More-López, María Isabel, García-del-Toro, Eva M., Alcala-Gonzalez, Daniel, García-Salgado, Sara, 2023. Sustainability assessment in infrastructure projects. Sustainability 15 (20), 14909. https://doi.org/10.3390/su152014909.

Moretti, L., Di Mascio, P., Bellagamba, S., 2017. Environmental, human health and Socio-Economic effects of cement powders: the multicriteria analysis as decisional methodology. Int. J. Environ. Res. Publ. Health 14 (6), 645. https://doi.org/10.3390/ijerph14060645.

Moro, C., Francioso, V., Lopez-Arias, M., Velay-Lizancos, M., 2022. The impact of CO_2 uptake rate on the environmental performance of cementitious composites: a new dynamic Global Warming Potential analysis. J. Clean. Prod. 375, 134155. https://doi.org/10.1016/j.jclepro.2022.134155.

Navarro, I.J., Villalba, I., Yepes-Bellver, L., Alcalá, J., 2024. Social life cycle assessment of railway track substructure alternatives. J. Clean. Prod. 423, 142008. https://doi.org/10.1016/j.jclepro.2024.142008.

Negrín, V., Kripka, M., Yepes, V., 2023. Multi-criteria optimization for sustainability-based design of reinforced concrete frame buildings. J. Clean. Prod. 425, 139115. https://doi.org/10.1016/j.jclepro.2023.139115.

Pakdel, A., Ayatollahi, H., Sattary, S., 2021. Embodied energy and CO2 emissions of life cycle assessment (LCA) in the traditional and contemporary Iranian construction systems. J. Build. Eng. 39, 102310. https://doi.org/10.1016/j.jobe.2021.102310.

Pascual-González, J., Guillén-Gosálbez, G., Mateo-Sanz, J.M., Jiménez-Esteller, L., 2016. Statistical analysis of the ecoinvent database to uncover relationships between life cycle impact assessment metrics. J. Clean. Prod. 112, 359–368. https://doi.org/10.1016/j.jclepro.2015.06.058.

Penadés-Plà, V., García-Segura, T., Martí, J.V., Yepes, V., 2018. An optimization–LCA of a prestressed concrete precast bridge. Sustainability 10 (3), 685. https://doi.org/10.3390/su10030685.

Polo-Mendoza, R., Martinez-Arguelles, G., Peñabaena-Niebles, R., 2023. Environmental optimization of warm mix asphalt (WMA) design with recycled concrete aggregates (RCA) inclusion through artificial intelligence (AI) techniques. Results Eng. 17, 100984. https://doi.org/10.1016/j.rineng.2023.100984.

Richardson, J., 2003. Precast concrete structural elements. In: Newman, J., Choo, B.S. (Eds.), Advanced Concrete Technology. Butterworth-Heinemann, Oxford, pp. 3–46.

Rostamnezhad, M., Thaheem, M.J., 2022. Social sustainability in construction projects—A systematic review of assessment indicators and taxonomy. Sustainability 14 (9), 5279. https://doi.org/10.3390/su14095279.

Ruiz-Vélez, A., Alcalá, J., Yepes, V., 2023a. A parametric study of optimum road modular hinged frames by hybrid metaheuristics. Materials 16 (3), 931. https://doi.org/10.3390/ma16030931.

Ruiz-Vélez, A., Alcalá, J., Yepes, V., 2023b. Optimal design of sustainable reinforced concrete precast hinged frames. Materials 16 (1), 204. https://doi.org/10.3390/ma16010204.

Sadafi, N., Zain, M.F.M., Jamil, M., 2012. Adaptable industrial building system: construction industry perspective. J. Architect. Eng. 18 (2), 140–147. https://doi.org/10.1061/(ASCE)AE.1943-5568.0000075.

Sánchez-Garrido, A.J., Moreno-Serrano, J.F., Navarro, I.J., Yepes, V., 2026b. Innovative safety framework and direct load–settlement method to optimize vertical subgrade modulus in sustainable mat foundations. Environ. Impact Assess. Rev. 118, 108191. https://doi.org/10.1016/j.eiar.2025.108191.

Sánchez-Garrido, A.J., Navarro, I.J., Yepes, V., 2022. Multi-criteria decision-making applied to the sustainability of building structures based on Modern Methods of Construction. J. Clean. Prod. 330, 129724. https://doi.org/10.1016/j.jclepro.2021.129724.

Sánchez-Garrido, A.J., Navarro, I.J., Yepes, V., 2026a. Optimizing reactive maintenance intervals for the sustainable rehabilitation of chloride-exposed coastal buildings with MMC-based concrete structure. Environ. Impact Assess. Rev. 116, 108110. https://doi.org/10.1016/j.eiar.2025.108110.

Su, S., Sun, A., Yan, H., Wang, Q., Li, L., Zhu, J., 2025. Optimization of construction program for economic and environmental sustainability. Renew. Sustain. Energy Rev. 208, 115006. https://doi.org/10.1016/j.rser.2024.115006.

United Nations Environment Programme (UNEP), 2022. Emissions Gap Report 2022: the Closing Window – Climate Crisis Calls for Rapid Transformation of Societies (Executive Summary). UNEP.

World Commission on Environment and Development (WCED), 2015. Transforming our World: the 2030 Agenda for Sustainable Development. WCED, New York, NY.

Yepes-Bellver, L., Alcalá, J., Yepes, V., 2025. Predictive modeling for carbon footprint optimization of prestressed road flyovers. Appl. Sci. 15 (17), 9591. https://doi.org/10.3390/app15179591.

Zajemska, M., Wojtyto, D., Michalik, J., Berski, S., 2025. Review of Current trends in sustainable construction. Energies 18 (10), 2559. https://doi.org/10.3390/en18102559.

Zhang, T., Zhu, R., Gao, S., 2026. Compressive behavior of coal gangue concrete-filled steel tube in cold region towards to sustainability design. Constr. Build. Mater. 506, 145002. https://doi.org/10.1016/j.conbuildmat.2025.145002.

Zhu, W., Li, J., Wang, L., Li, X., 2025. Sustainable design of recycled concrete using shape optimization and carbon dioxide emission based on LCA. J. Civ. Eng. Manag. 31 (6), 631–645. https://doi.org/10.3846/jcem.2025.24108.

Zulu, K., Singh, R.P., Shaba, F.A., 2020. Environmental and economic analysis of selected pavement preservation treatments. Civil Engineering Journal 6 (2), 210–224. https://doi.org/10.28991/cej-2020-03091465.